COMPARISON OF SIDE EFFECTS OF ANTI-CANCER DRUGS IN 2D AND 3D, CLASSICAL AND CELL-ON-A-CHIP CULTURES

A Thesis Submitted to
The Graduate School of Engineering and Sciences of
Izmir Institute of Technology
in Partial Fulfillment of the Requirements for the Degree of

MASTER OF SCIENCE

in Biotechnology and Bioengineering

by
Deniz KANKALE

July 2016
IZMIR

We approve the thesis of **Deniz KANKALE**

Examining Committee Members:

Assoc. Prof. Dr. Devrim PESEN OKVUR
Department of Molecular Biology and Genetic, Izmir Institute of Technology

Assoc. Prof. Dr. Hüseyin Çağlar KARAKAYA
Department of Molecular Biology and Genetic, Izmir Institute of Technology

Assoc. Prof. Dr. Özlem YEŞİL ÇELİKTAŞ
Department of Bioengineering, Ege University

29 July 2016

Assoc. Prof. Dr. Devrim PESEN OKVUR
Supervisor, Department of Molecular Biology Genetic, Izmir Institute of Technology

Assoc. Prof. Dr. Ali ÇAĞIR
Co-Supervisor, Department of Chemistry, Izmir Institute of Technology

Prof. Dr. Volga BULMUŞ
Head of the Department of Biotechnology And Bioengineering

Prof. Dr. Bilge KARAÇALI
Dean of the Graduated School of Engineering and Sciences

ACKNOWLEDGEMENTS

I would like to thank to advisor Assoc. Prof. Dr. Devrim PESEN OKVUR for her encouragement, understanding, guidance and support throughout this study.

I am thankful to co-supervisor Assoc. Prof. Dr. Ali Çağır and the members of my thesis defense committee Assoc. Prof. Dr. Özlem YEŞİL ÇELİKTAŞ and Assoc. Prof. Dr. Hüseyin Çağlar KARAKAYA.

I would like to thank to The Scientific and Technological Research Council of Turkey for financial support (231M668).

I would like to express my deepest appreciation and thanks to my friends and colleagues Gizem BATI and Berrin ÖZDİL for their support, help and friendship.

I am very thankful to the members of the Controlled *in vitro* Microenvironments (C*iv*Ms) laboratory for their team spirit and support.

I would like to thank also Irmak KAYSUDU and Deniz UĞUR for their help and encouragement.

I would like to thank to especially Can BAŞALOĞLU for his love, understanding and support.

Finally, I would like to express my love and missing to my grandmother, father and mother hope to always see and be with me.

ABSTRACT

COMPARISON OF SIDE EFFECTS OF ANTI-CANCER DRUGS IN 2D AND 3D, CLASSICAL AND CELL-ON-A-CHIP CULTURES

The studies that aim to assess the effects of drugs developed against cancer at the cellular level use multiwell plates. However, these classical systems fail to reproduce the *in-vivo* like microenvironment necessary for realistic assessment. In addition, classical cell culture systems use high amount of materials increasing cost. On the other hand, lab-on-a-chip systems use minimal volumes of reagents and more importantly can mimic the *in-vivo* microenvironment via spatial and temporal control. Furthermore, it is known that cell response to drugs can be very different in 2D and 3D cell culture setups. Doxorubicin is a widely used anticancer drug. Here, doxorubicin uptake by highly metastatic human breast cancer cell line MDA-MB-231 and normal mammary epithelial cell line MCF10A were investigated using 2D and 3D, classical and cell-on-a-chip cultures. Drug uptake at 24, 48 and 72 hours various concentrations of the drug determined by measuring signal intensities from fluorescence microscopy images of cells. For cell viability assay, cells were stained with dapi and two cell lines were compared in systems. According to results, it was observed that 3D cell culture environment in chip provides more *in-vivo* like environment with less reagent consumption and cell viability is not correlated only with drug uptake.

ÖZET

KANSERE KARŞI İLAÇLARIN YAN ETKİLERİNİN 2B VE 3B, KLASİK VE ÇİP-ÜZERİ-HÜCRE KÜLTÜRÜNDE KARŞILAŞTIRILMASI

Kansere karşı geliştirilen ilaçların etkilerinin incelenebilmesi için hücresel düzeyde yapılan çalışmalar çoklu kuyucuklar kullanılarak yapılmaktadır. Ancak bu klasik sistemler gerçekçi denemeler için gerekli *in-vivo* benzeri mikroçevre oluşturmakta başarısız olmaktadırlar. Ayrıca klasik hücre kültürü sistemleri artan maliyetlerle yüksek miktarda malzeme kullanmaktadır. Diğer yandan çip-üzeri-laboratuvar sistemleri minimum reaktif hacmi kullanmakta ve daha önemlisi *in-vivo* mikroçevreyi boyutsal ve zamansal taklit edebilmektedir. Dahası hücrelerin ilaca karşı karşılıklarının 2B ve 3B hücre kültürü denemelerinde değiştiği bilinmektedir. Doksorubisin yaygın olarak kullanılan bir antikanser ilacıdır. Bu çalışmada, yüksek oranda metastatik insan meme kanseri hücre hattı MDA-MB-231 ve normal meme epitel hücre hattı MCF10A tarafından ilaç alımı 2B ve 3B, klasik ve çip-üzeri-hücre kültüründe araştırılmıştır. Farklı ilaç dozlarının 24, 48 ve 72. saatlerde alımı hücrelerin floresan mikroskobundaki resimlerinden sinyal yoğunluğu ölçülerek hesaplanmıştır.Hücre canlılığı analizi için hücreler dapi ile boyanmış ve iki hücre hattı bu sistemler içerisinde karşılaştırılmıştır. Sonuçlara göre, çip içerisindeki 3B hücre kültürü ortamın daha az reaktif tüketimiyle birlikte daha çok *in-vivo* benzeri ortamın sağladığı ve hücre canlılığının sadece ilaç alımıyla orantılı olmadığı gözlenmiştir.

To my family…

TABLE OF CONTENTS

LIST OF FIGURES

LIST OF TABLES

CHAPTER 1

INTRODUCTION

1.1. Cancer

Cancer is the major disease to cause morbidity and mortality around the world (Siegel, Naishadham, & Jemal, 2012). According to the WHO, cancer resulted in death about 8.2 million people in 2012 and the number is expected to increase within decades. This disease is basically caused by the abnormal proliferation of cells in any parts of the body, while normal tissues have defined boundaries. Cancer cells pass the boundary of the growth in tissue due to the mutations in the DNA structure and repress the tumor suppressor genes, therefore, escape from the apoptosis and stimulate angiogenesis with metastasis (Esmaeilsabzali, Beischlag, Cox, Parameswaran, & Park, 2013; Joyce & Pollard, 2009).

1.1.1. Breast Cancer

Breast cancer is the multi-sourced disease, assorted with different determinants as histopathological classification as lobular or ductal and receptor protein expression as endocrine receptor (Lovitt, Shelper, & Avery, 2015). Metastasis is the progress that one or more cancer cells migrate from primary cite, enter the circulation system and invade endothelial barrier, then settle in a secondary cite (Fidler, 2003). According to the progression of the disease, breast cancer is the metastatic as among 8 patients 1 of them has metastasis (Bar-On, Shapira, & Hershko, 2007). Breast cancer is seen both gender both dominantly arises in female. In 2012, a quarter of the cancer cases are consisted from the female breast cancer patients (Ferlay et al., 2015).

1.2. Drug Discovery

Drug discovery is an increasing area of the marketing, but the success of the drug at the clinical level is significantly low. The low efficiency, inadequate pharmacokinetics, poor pre-clinical data from both cell culture and *in vivo* model trials and high adverse effects decrease the marketing stage of the success (Lee et al., 2008a; Singh, 2006).

Although the complexity and heterogeneity of the diseases is known, *in vitro* and *in vivo* studies can only take into account several ways of the disease conditions. *In vitro* experimental setups are the minimalist in nanoscale constructions in order to identify the basis of the diseases and display of the idea of diseases occurrence. *In vitro* conditions especially in 3D conditions are important for drug testing in cancer models, because % 95 of the drugs are unsuccessful in clinical trial wile effective in *in vitro* conditions (Hickman et al., 2014). The main reason for the low rate success is the 2D model cell culture inefficiency to demonstrate *in vivo* conditions (van de Waterbeemd & Gifford, 2003). The response of drug in 2D and 3D is different due to the phenotypic change of the cells, and diffusion rate of the drug in the system. In pre-clinical drug screening 3D modeling of the drug delivery is potentially the key setup for the bioengineers (Lee et al., 2008b).

Proper in vitro conditions can control pH, nutrients and oxygen in the system and this can be performed with proper designed 3D culture system (Hickman et al., 2014).

In 3D system, matrix proteins and the pore size is important for the diffusion of drug during treatment (Goodman, Ng, & Pun, 2008). In some case cancer patients have resistance to drugs, called as multidrug resistance (Wartenberg et al., 1998; Zhau, Goodwin, Chang, Baker, & Chung, 1997; Zhu et al., 2005; H Zhu et al., 2012). The activity of multidrug resistance is increased in case of hypoxia, low pH and low growth factors (Milane, Duan, & Amiji, 2011; Webb, Chimenti, Jacobson, & Barber, 2011; Wei & Roepe, 1994; Xu, Sabanayagam, Harrington, Farach-Carson, & Jia, 2014; H. Zhu et al., 2012),

1.3. Doxorubicin

Doxorubicin (Dox) is an anthracycline antibiotic commonly used chemotherapeutic agent in treatment of various cancer types (Kenny et al., 2007; Lown, 1993). It has antineoplastic activity and sourced from the bacterium Streptomyces peucetius var. caesius. It can be used for treatment of various cancer types such as: malignancies like leukemia and lymphoma, many types of carcinoma like breast cancer or soft tissue sarcomas like osteosarcomas.

The antitumor activity of doxorubicin has been attributed to its intercalation into the nuclear and mitochondrial DNA, the production of reactive oxygen species and the inhibition of topoisomerase II. This inhibition causes the breaks on the DNA strand and leads to cell death.

Severe breast cancer is treated with anthracycline and taxane. Anthracycline inhibits topoisomerase II so the replication of the cell, taxane binds to microtubules that inhibit growth of the cell and division of the cells. Studies show that the drug efficiency is changing in 2D and 3D systems and also the efficiency is depending on the drug and cell line (Nicolini et al., 2006).

1.4. 2D versus 3D Cell Culture

Experimental design of cell culture systems *in vitro* generally contains 2D system, which depends on the monolayer cultured cells on polystyrene or glass substrates. In 2D system, all cells equally reach the oxygen and factors included in their medium, however, *in vivo* cells face with molecules in gradient (Mehta, Hsiao, Ingram, Luker, & Takayama, 2012). Because the aim of these experiments is mimicking *in vivo* condition, 2D systems are not adequate at some point. 2D system suggests idea about the developmental biology, tissue morphogenesis, disease mechanisms, drug discovery and so on (Xu, Farach-Carson, & Jia, 2014). The actions of the molecules at some point are deactivated in 2D system; because of that, 2D results in some case cannot be interpreted for *in vivo* (Goodman et al., 2008). *In vitro* experiments should include parameters that are not found in 2D system, such as extracellular matrix (Toplin, 1959). Extracellular matrix gives one extra dimension and called as 3D cell culture system in experimental design (Hutmacher, 2010; Hutmacher et al., 2010).

3D cell culture system is the stage between 2D system and *in vivo* system; better mimicking *in vivo* conditions and revealing different processes and application of different chemicals especially in cancer studies 3D cell culture systems are a hot topic for a decade (Breslin & O'Driscoll, 2013).

2D cell culture system is lack of cell-cell and cell-matrix interaction demonstrations that are required in cancer progression and metastasis studies. However, in 3D cell culture system, like *in vivo* conditions these interactions can be traceable (Godugu et al., 2013; Kang, Chung, Langer, & Khademhosseini, 2008). In addition to this, 3D cell culture systems have preliminary data for clinical applications when compared to 2D systems (Lovitt et al., 2015). In 2D systems drug screening shows the basis of the action of the drug, but when applied in clinics, mostly drug efficiency is not appropriate (Ferlay et al., 2015). *In vivo* studies should be performed to confirm 2D and 3D system results, however, because *in vivo* studies are performed in limited number due to the ethical issues, importance of the 3D system increases at that point (Godugu et al., 2013; Nguyen, Shaegh, Kashaninejad, & Phan, 2013).

The reason of the 3D cell culture system is better mimics the *in vivo* is because *in vivo* cells are surrounded with the matrix and interacts their neighboring cells though the extracellular matrix both mechanical and chemical interactions in gradient fashion (Jaeger et al., 2013; Placzek et al., 2009). The biological processes are determined by the extracellular matrix (Bissell, Radisky, Rizki, Weaver, & Petersen, 2002). In order to construct 3D system, cell biologist, biomedical engineers, material scientist and other contributors work together to the best *in vitro* model (Sanyal, 2014).

3D culture system includes extracellular matrix, which varies in different condition and various diseases. Mostly used extracellular matrix is matrigel, which is a company product, contains collagen type IV, laminin, perlecan, entactin and several growth factors; isolated from Engelbreth–Holm–Swarm (EHS) mouse sarcoma (Hall et al., 2008; Lovitt et al., 2015; Menke et al., 2001).

Collagen type I is another commonly used material in biological research. *In vivo* it is mainly found in bone and stroma. It is isolated from rat tail, human placenta and bovine skin. Collagen is the most abundant protein in extracellular matrix, it has fibrous structure. Collagen can interact with transmembrane protein integrin that both provide adhesion and activation of signaling pathways (Kiefer & Farach-Carson, 2001).

Natural matrices can have disadvantages at some points. The components are isolated from the animals, therefore the ingredients can vary. In addition to that, because

sourced from the animal species dependent studies need advanced materials (Sanyal, 2014).

Experiments with extracellular matrix also can be used in 2D cell culture system with using extracellular matrix as a coating material. The surface that is used for the adherence of the cells can be coated with one of the extracellular matrix component (such as fibronectin) or protein rich mixture (matrigel). However, in 3D system cell is surrounded with any of the extracellular matrix components. In these two experimental setups, beside the ingredient difference, stiffness is the one of the major role to influence the cell fate in these cell culture systems. The effect of the stiffness on stem cell is showed that, only by changing the substrate stiffness, stem cell differentiation can be controlled (McBeath, Pirone, Nelson, Bhadriraju, & Chen, 2004; Park et al., 2011). Moreover, in cancer cell invasion and drug testing experiments, matrix stiffness is an important parameter that can change slightly the results (Levental et al., 2009; Pathak & Kumar, 2012; Schrader et al., 2011; Soman et al., 2012; Zustiak, Nossal, & Sackett, 2014). Stiffness of 2D cell culture system is 1-2 GPa while normal breast tissue is 160 Pa, and breast cancer tissue is 4kPa. Commonly used extracellular matrix stiffness is approximately 200-400 Pa (Correia & Bissell, 2012). Different substrate in different experimental setups activate various signaling pathways and differentiate the phenotype of the cells (Aoudjit & Vuori, 2001; Danen, 2013; Huang et al., 2011; Menendez et al., 2005; Sethi et al., 1999). The differential protein expression through the activation of signaling pathway changes the angiogenic activity, cell motility, and drug sensitivity (Carpenter et al., 2009; Languino et al., 1989; Miyamoto et al., 2004; Zhou et al., 2004).

In 3D culture, while matrix surrounds the cells, cells also contribute and adhere to gels, absorb and secrete molecules into the gel while changing the gene and protein expression (Kenny et al., 2007). Matrix gel used in 3D system is expensive that limits large scale trials (Sodunke, Turner, Caldwell, McBride, & Reginato, 2007), however, miniaturize and automated nano-scale systems is appropriate for cancer progression and drug tests (Lovitt et al., 2015).

1.5. Lab-on-a-chip

LOC (Lab on a chip) is the device contains the whole laboratory on a single micro-scale device. This has several advantages and can be used in several areas. In

biological applications, LOC is used in cell culture, drug delivery and sample handling (Westwood, Jaffer, Lui, & Gray, 2007). Because the device is in micrometer scale, sampling volume is in micro liter and even nano liter scale. In order to prepare LOC system, several methods can be used and one of them is photolithography. Photolithography is performed on the glass or silicon substrate. In order to gain the desired design, photolithography steps can be modulated and transferred to a bioappliable polymer molds.

Modulation can be made according to the cost, biocompatibility, transparency, and simplicity of the fabrication (Bélanger & Marois, 2001). Silicon is widely used in photolithography method and SU-8 is used as a photoresist. The common molding polymer is polydimethylsiloxane (PDMS) in LOC construction (Xia and Whitesides 1998). The advantages of LOC system is list in Figure 1. The main advantage of the LOC system is the small size, therefore the used material and the waste products are also in small volume. Because of the transparency of the LOC, device can be monitored under the microscope and because of the small size it can be transported away from the fabrication site. LOC system can be used in both 2D and 3D experimental designs, so that according to the desired conditions, it can be modulated both in chemical ingredients and design of the mold.

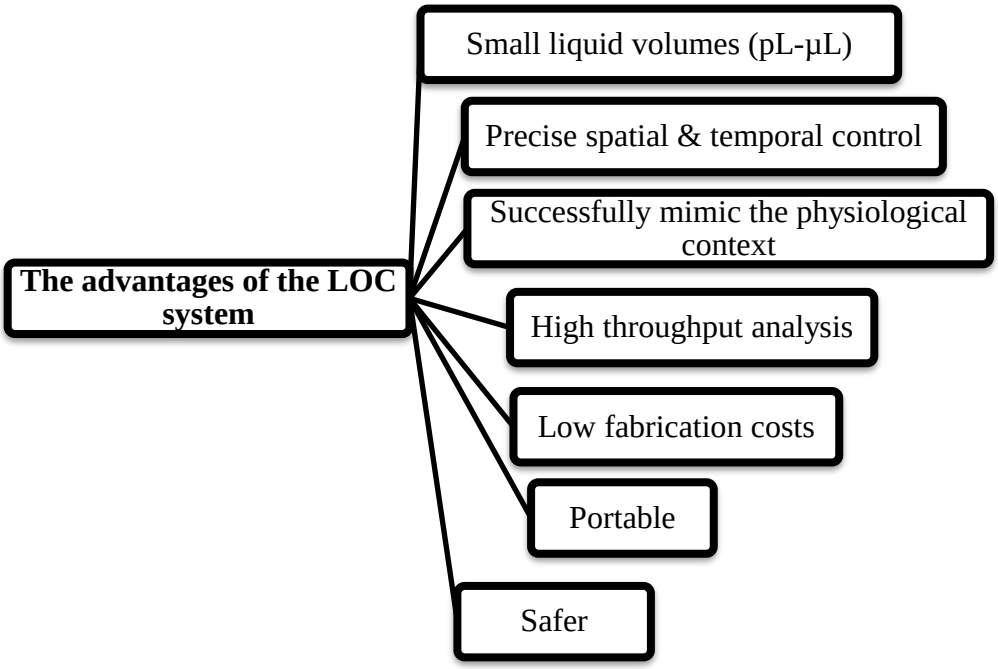

Figure 1.0.1. The list of advantages of LOC system

LOC systems can be used as microfluidic devices, also can be named as micro bioreactors (Nguyen et al., 2013). Drug testing with microfluidic devices is a developing area with high throughput (Tsui, Lee, Pun, Kim, & Kim, 2013). Conventional studies optimize the drug testing but bulk of the reagents are used with long time experimental setup, however, with the microfluidic devices decreases the reagent and time used during drug testing (Smith, 2007; Whitesides, 2006). Microfluidic devices are attached with the flow system with parallel setup that the flow rate can be adjusted according to the experimental setup (Beebe, Mensing, & Walker, 2002). However, these systems are not compatible with complexity have scale limitations (Hickman et al., 2014). Microfluidic devices supply the study of cancer progression, angiogenesis and metastasis (Zhang & Nagrath, 2013). In microfluidic devices because the enterance and exit of the solutions are controlled by the researcher, spatio-temporal changes can be easily controlled (Sackmann, Fulton, & Beebe, 2014). Microfluidic devices handle many studies including single cell analysis to flow cytometry; has a big impact on the identification unclear points of biology (Paguirigan & Beebe, 2008).

LOC systems are recently developed according to the need of clinical drug treatments. Because of this need, LOC is tried to be a organ on a chip devices. The advance form of this LOCs are the human on a chip (Huh, Hamilton, & Ingber, 2011). These developments are done in order to identify the functions of any factor in vivo that has effects in drug therapies. The organ on a chip studies continue as lung on a chip (Huh et al., 2010), blood vessel on a chip (Bischel, Young, Mader, & Beebe, 2013; Song & Munn, 2011; Tsai et al., 2012), cancer on a chip (Sung et al., 2011; Walsh et al., 2009; Zervantonakis et al., 2012), and so on.

Production of LOC requires expensive infrastructure. Custom LOC systems also need much more effort to be optimized (Ghallab, 2010). For cell culture studies, one also has to take into account any absorption of hydrophobic molecules, any deviations from normal growth due to high surface to volume ratios and limited culture volumes.

CHAPTER 2

MATERIALS AND METHODS

2.1. Cell Culture

2.1.1. MDA-MB-231 Culture Medium Preparation

A day before the preparation of the culture medium, 50 ml fetal bovine serum, 5 ml L-glutamine and 5 ml Pen-step aliquotes were taken from +4°C to -20°C. The preparatory stage took place in a laminar cabinet. DMEM high glucose containing 500 ml of serum-free medium was obtained as a company. 50 ml DMEM high glucose was separated and was stored +4°C. Therefore remaining solution (450 ml DMEM high glucose) and 50 ml fetal bovine serum was mixed in order to provide 1:10 ratio. L-glutamine and Pen-strep solutions were added to this mixture. The bottle was rotated up-side down about 10 times and filtred with PES filter system. MDA-MB-231 medium was stored at +4°C.

2.1.2 MCF10A Culture Medium Preparation

A day before the preparation of the culture medium, 50 ml donor horse serum, 5 ml L-glutamine and 5 ml Pen-step aliquotes were taken from +4°C to -20°C. The preparatory stage took place in a laminar cabinet. DMEM-F12 containing 500 ml serum-free culture medium was supplied from the company. 25 ml of donor horse serum aliquots were prepared previously into 50 ml falcons. 12-13 ml DMEM-F12, Pen-strep, L-glutamine were added into this 50 ml falcon. 250 microliters hydrocortisone (stored at -20°C), 500 microliters insulin (stored at -20°C) and 50 microliters choleratoxin (stored at +4°C) were added to falcon. Finally, 100 microliters epidermal growth factor (stored at -80°C) was added to mixture. Then, this mixture was transferred to DMEM-F12 bottle. The bottle was rotated up-side down about 10 times and filtred with PES filter system. MCF10A medium was stored at +4°C.

2.1.3. Passage of MDA-MB-231 and MCF10A

The cells were checked under a microscope prior to the passage. If the confluency was 80 to 90% of surface area, cells were passaged. Laminar cabinet was sterilized prior to passage. All things taken into the cabinet were sterilized with 70% ethanol. Before use, trypsin-EDTA solution and the culture medium taken to room temperature from +4 ° C. Cells were grown on 100 mm petri dishes. Petri dish was placed into laminar cabinet and medium was aspirated and 2 ml trypsin-EDTA solution was added. This step was performed in order to discared former medium. Trypsinsin-EDTA solution was aspirated and in order to detach the cells from the petri dish surface, 4 ml tyripsin-EDTA soluiton was added. Petri dish was placed into incubator 3 minutes for MDA-MB-231 and 17 minutes for MCF10A. During this period of time, 10 ml fresh medium was transferred to new petri dish and placed into incubator. 15 ml falcon was placed into rack. After the required time finished, cells were inspected under microscope; cells became rounded shape and most of them were float. Bottom and sides of the petri dish were slightly hit in order to detach cells from surface completely and observed under microscope. After that, petri dish was taken into laminar cabinet and in order to inactivate the trypsin-EDTA solution 1 ml medium (which contains serum) was added. This 5 ml solution was pipetted up and down to separate cells from surface and solution was transferred to 15 ml falcon. 5 ml fresh medium was transferred to petri dish and pipetted up and down, then added to the falcon. Petri dish was observed under microscope and discared to the cell culture waste. 15 ml falcon was centrifugated at 1000 rpm for 5 minutes. Solution part was aspirated with vacuum and pellet was dissolved in 1000 microliters medium. For cell counting, 90 microliter medium and 10 microliter cell solution were mixed into tube (1:10 dilution). Dissolved cell pellet was separated according to the desired ratio, and transffered to the pre-warmed medium placed into incubator before. Petri dish was moved X-Y direction in order to separate cell uniformly through the surface. Petri dish was placed into incubator. Passage procedure was performed each 2-3 days.

2.1.4. Cell Freezing

MDA-MB-231 cell seeded at the ratio of 1/2 and MCF10A cells of 1/4 reached 80-90% confluency into two days were lifted from the petri dish surface and after centrifugation, pellets of these cells were dissolved in 1000 microliters fresh medium. During cells freezing process, DMSO (dimethyl sulfoxide) was used as cytoprotectant in order to avoid water molecule damage into the membrane. DMSO solution was prepared as it was 5% of the total volume of 1000 microliters. 1000 microliters %5 DMSO in culture media was added dropwise slowly to in the other tube that contained 1000 microliters cell dissolved culture medium in order to avoid any shock to the cells. 2000 microliters of total volume was placed in two cryo tube as 1000 microliters to each. Cells were placed at -80 ° C in isopropanol container that supplied stepwise freezing without shocking the cells. After 24 hours cryotubes were removed to liquid nitrogen tank.

2.1.5. Cell Thawing

After equlibration of water bath at 37 ° C, previously frozen cells in cryo tubes were taken from the liquid nitrogen tank. Until the solution was thawed, the cryotube was holded as half of the tube was into the water. 1 ml of dissolved cells were transfered into 9 ml of culture medium and centrifugated in order to remove cryoprezervation chemical (DMSO). Cells were dissolved in 1000 microliters culture medium, and transferred to the pre-warmed 10 ml culture medium previously put into incubator. After 24 hours, the culture medium of cells was changed. Culture medium of the cell was changed every two days until cells covered the surface and were ready to the passage. Thawed cells were used in the experiments after at least two passages passed.

2.1.6. Cell Counting

The cells were dissolved in 1 ml culture medium after passage and diluted 1:10 ratio for cell count. Before loading the hemocytometer (as shown in Figure 2.1) cells were pipetted in order to detach from each other. Cells were observed with phase-contrast microscope after loading. Number of cells existing on four separated area of hemocytometer counted and collected. Number was divided into four in order to find average cell number and multiplied by dilution factor (1:10). Then it was multiplied by the correction factor. Cell number of MDA-MB-231 into the 100 mm petri dish was calculated approximately 6 millions cells / ml, whereas MCF10A cells was 10 millions cells / ml.

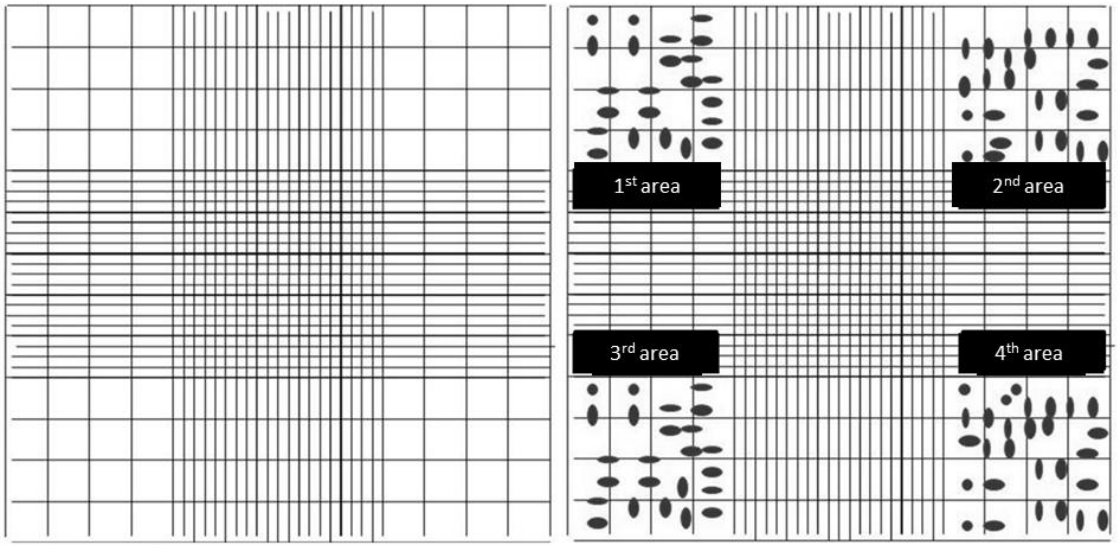

Figure 2.1. Example of cell number calculation
(number of cells in 1st area + 2nd area + 3rd area + 4th area) / 4 × dilution ratio × 10^4 = number of cells per mililiter)

2.2. Chip Preparation

2.2.1. UV Lithography

UV lithography process on the first day included pouring SU-8 photoresist on silicon surface, spreading this solution, rotation with spinner for uniform distribution and baking. UV lithography process began on the second day with baking steps performed by measuring adequate baking test of the first day with wrinkle test. Then mask containing desired design was placed on the sample and a sample was exposed to UV light at the time set. After exposed to UV light, sample was heated and allowed to cool until the next day. On the third day, the sample was put into solution called developer and uncrossed areas of the sample were discarded. SU-8 mold was finally washed with isopropanol and dried, the mold was ready for use. For the production of PDMS molds, SU-8 molds, which were fabricated with UV lithography method, were used.

Silicon surface was used for UV lithography method; because the silicon surface was more suitable for SU-8 based polymers bonding than the glass substrates. The heater was set primarily in 65ºC and silicon wafers were placed on the heater at 65° C for about 5 minutes. This waiting step provided SU-8 spread faster which then be poured onto the silicon surface. Approximately 4 ml of SU-8 was slowly poured onto the heated silicon layer and spread onto the substrate. Roughly spread SU-8 was evenly spreaded with the 'spinner' machine. According to the value entered in this machine, such as how fast the rotation stage how long it will rise, how much time to be return at this speed and stopped at the time was determined. The values shown in Table 2.1 was applied in this study and indicated heights obtained accordingly. The hight of the channels depended on the rotation of the intermediate stages but also depended SU-8 amount used in the casting step.

Thickness	Spin time	Spin speed	Spin time	Spin time	Spin speed	Spin time	Spin time	Spin Speed
100 µm	10 seconds	500 rpm	45 seconds	5 seconds	1000 rpm	30 seconds	5 seconds	0 rpm
185 µm	5 seconds	500 rpm	10 seconds	5 seconds	1000 rpm	20 seconds	5 seconds	0 rpm

Table 2.1. Thickness resulting from varying spin and speeds for SU-8 mold preparations.

After the spin step, the sample was placed in 65°C for 5 minutes and then heater was adjusted to 95°C. The sample was maintained at this temperature for 30 minutes. Then, the heater was turned off and the sample was allowed to cool for a day. SU-8 photoresist was sensitive to sudden changes in temperature and sudden temperature changes could cause cracks and fractures in the mold. On the second day of UV lithography, sample was allowed to stand at room temperature. Meanwhile, the heater was set to 95ºC. When the heater has reached the desired temperature, the sample was placed on heater and SU-8 surface was inspected to identify whether there were wrinkles or not. Sample with wrinkles was baked for 5 minutes further and kept at room temperature. Then, the process repeated until eliminate wrinkles. After this step, the heater was set 65ºC. The sample was allowed to stand at room temperature. Sample loading part of the UV mask aligner was controlled with water balance, because the UV light should infuse SU-8 surface at the same level. Thereafter, the sample was placed and additional vacuum button was activated. Designed mask was placed on the sample as bright face at the top and written part at the bottom touching to the sample. UV light was applied at the indicated doses for 30 seconds. After exposure step, sample was placed on preset and equilibrated 65ºC heater. After 5 min, heater was adjusted to 95ºC and sample was held for 10 minutes at this temperature. Then, the heater was turned off and sample was allowed to stand until the next day on the heater. On the third day of UV lithography, sample was kept in developer for 5 minutes without shaking. Later, sample was kept in the same solution for 5 minutes with shaking. Then, the completion of development step was tested with isopropanol. For this, isopropanol was dropped at the corner of the sample. When the solution turned white, development step continued. When it was not white, sample was passed from the developer solution for SU-8

residual removal. In order to stop developer solution effect, sample was cleaned with isopropanol. The sample was dried with dust-free wipes and used for PDMS casting.

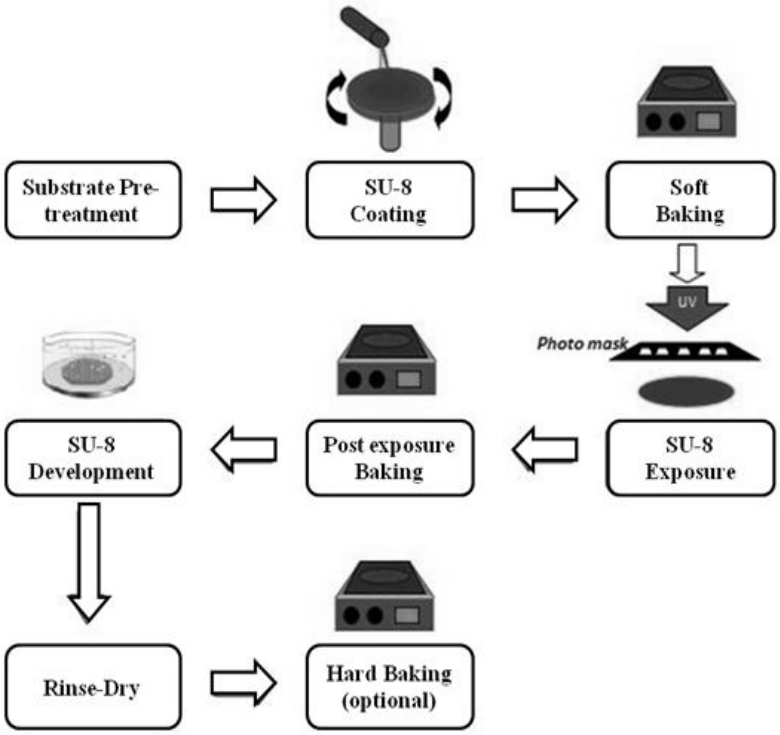

Figure 2.2. Overview of UV lithography technique
(Source: Murat Sağlam, 2014)

2.2.2. PDMS Molding

SU-8 molds produced were used for the production of PDMS molds. SU-8 molds could be used again and again; PDMS molds but were disposable. To prepare PDMS mold, PDMS Sylgard 184 PDMS elastomer base and curing agent were mixed by weight of 10: 1 ratio. In the resultant mixture, to eliminate the abundant bubbles formed, the mixture was kept under vacuum until all bubbles were resolved. PDMS mixture was poured onto the SU-8 mold and was kep two days at room temperature or one day 25^{o}C in oven. After PDMS polymer solidifies, it was removed from the SU-8 mold with the aid of 70% ethanol . PDMS mold was cut properly and loading points that was drilled with a variety of punches. Punches provided to create loading spots with different diameters and facilitated flow during loading.

2.2.3. PDMS Molds Cleaning and Sterilization

PDMS molds were passed through a cleaning stage prior to use. PDMS molds were washed with ultra pure water and treated with 70% ethanol. To resolve the ethanol residues, they were cleaned with ultra pure water. After this first cleaning step, the molds placed the containers sequentially in ethanol and ultra pure water and kept into sonicator. Removal of any substances from PDMS molds was provided with sonication. Then, the molds were allowed to dry at room temperature for 2 days.

2.2.4. Permanent Bonding and Sterilization

In order to clean slides, they were kept into methanol and ultra pure water and then dried. PDMS molds and slides were permanently bonded with each other after exposed UV/ozone for 5 minutes. They were placed on 100^{o}C heater and incubated for 10 minutes. This heating allowed the PDMS mold and the glass surface is permanently connected. Also UV / ozone step provided surfaces free from organic molecules. Surface that exposed to UV/ozone had hydrophilic surface. In preparation step this property was the negative feature for multi channel LOC, especially in loading step. LOCs to be used in cell culture studies were placed into laminar cabinet and exposed to UV light for 30 minutes. Then, they allowed to stand ready for use at room temperature.

2.2.5. Channel Height Measurements

Height of the channels were measured by ImageJ program. For this, first PDMS was poured to the SU-8 mold and waited for polymerization. From the polymerized mold, thin section was obtain. This section contained both the channel inside and outside border. Later this pattern was inspected under phase contrast microscope with a 4X objective. With the same objective, ruler was imaged as used scale for further measurements. Long bars spaced 1 mm, while short bars spaced 200 micrometers on ruler. These small bar space as pixel unit provided pixel to micrometer conversion.

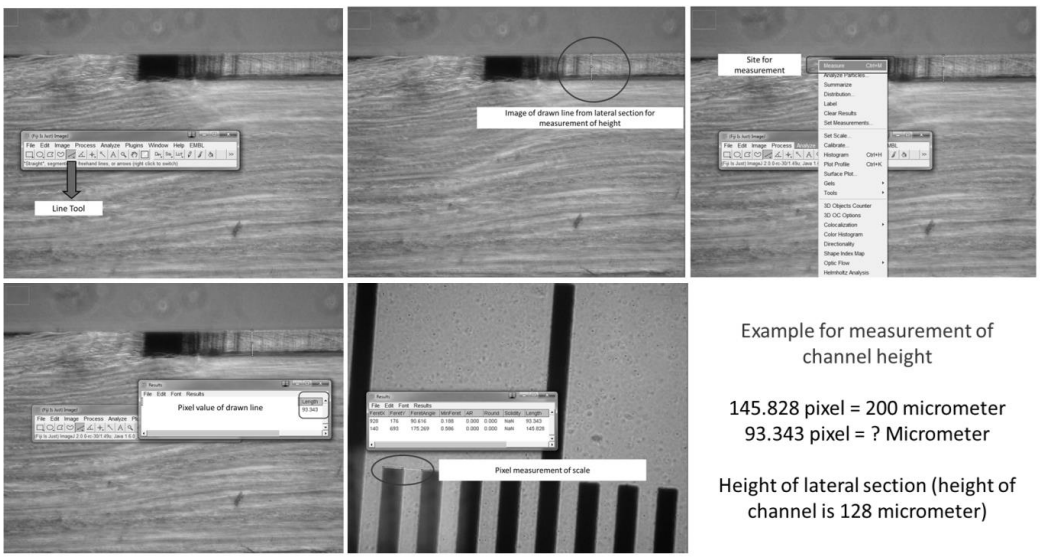

Figure 2.3. Example for calculating channel width

2.2.6. Image Analysis

ImageJ analysis software was used for image analysis. Phase-contrast and florescence images of doxorubicin at 555 nm emission wavelength of cells were taken. RGB format images of fluorescent microscope were split into color channels. Images were taken 16-bit format from microscope. ROIs were obtained by drawing cells from their phase-contrast images. Background values were measured in non-cell occupied areas by opening ROIs on florescent images and obtaining those non-cell obtained areas. The measured background values were subtracted from florescent images using Process>Math>Subtract steps. By applying ROI on background subtracted florescent images and excel formats were produced. Graphs were drawn using values obtained from dividing total integrated density to total area for every slice.

CHAPTER 3

RESULTS AND DISCUSSION

3.1. Channel Fabrication for 2D Experiments with UV Lithography Method

SU-8 mold was fabricated with UV lithography technique. The height of channel was 100 micrometers and the width of channel was 1 cm. In order to prepare the two-dimensional LOC, an air outlet hole in the middle of the channel and one each loading hole on each side of the channel were opened. UV / ozone exposure was used to stick to reservoir on the top of the channel, which supplied additional culture medium.

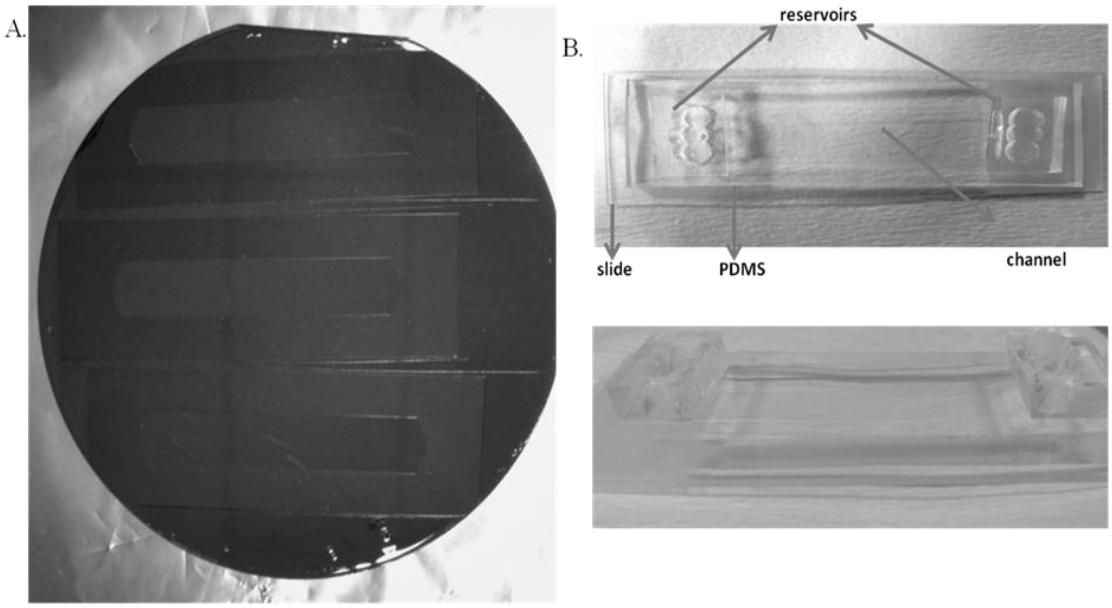

Figure 3.1. A. SU-8 mold prepared with UV lithography technique
B. LOC system for 2D experiments

3.2. LOC Preparation with Magnetic Paper for 3D Experiments

LOC system used for 3 dimensional trials was prepared with magnetic paper. It was aimed to use smaller amounts of matrigel and cell while preparing high numbers of

LOC. For this, a system that has an output of 22 LOCs was prepared by sticking magnetic papers with 150µm length and 50µm width. PDMS mixture was prepared and poured onto the mold and polymerized for two days at room temperature. After polymerization, PDMS mold was separated from magnetic paper with the use of ethanol and LOCs were cut off. 5mm diameter holes for reservoir and 1mm diameter holes for loading was opened using puncher. Cleaning was done using ultra pure water and 70% ethanol with sonicator and left to dry for 24 hours. 2 or 3 PDMS molds per glass slide were bonded using UV-ozone and heater.

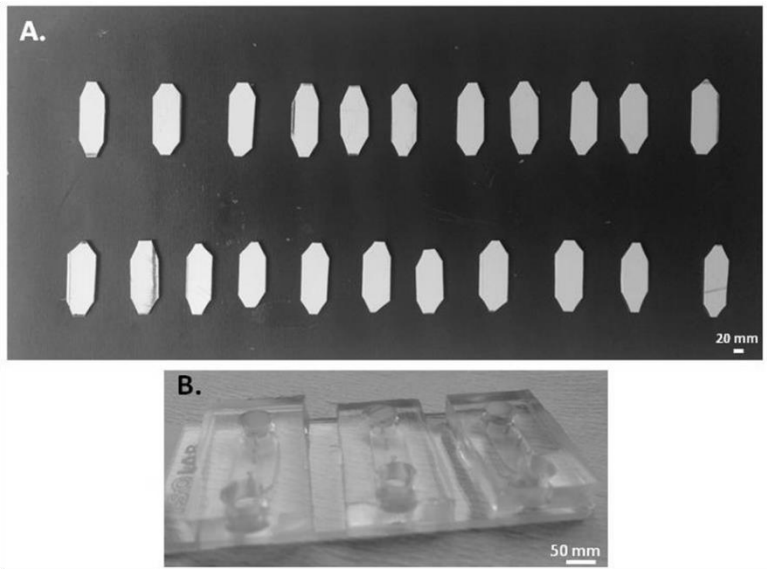

Figure 3.2. A. Mold prepared with magnetic papers B. LOC system for 3D experiments.

Cells were added to LOC system mixed with matrigel in order to produce 3D environment. 6 millions per mililiter MDA-MB-231 and MCF10A cells were mixed with matrigel with the ratio of 1:1 and added to the system with the final concentration of 3 millions. In order to polymerize them, they were incubated at 37°C at 5% CO_2 upside down for 30 minutes. MCF10A medium was added to the reservoirs for both cell lines and incubated for two days in order to prepare for experimentation.

3.3. Surface Modification and Optimization of Cell Culture for 2D Lab-on-a-chip System

Observation of cells using an upright microscope required that cells were attached to the PDMS ceiling of the cell-on-a-chip. Cells adhere normally on glass surface, but not the PDMS surface. Cell-on-a-chips housed inlets and outlets at the PDMS part for loading and to accomodate tubing for possible flow experiments. Thus cell-on-a-chips could not be used upside-down to overcome the limitations of an upright microscope. Therefore a protocol was developed that allows cell adhesion on the PDMS surface.

In order to promote cell adhesion on PDMS surface, PDMS molds were coated with poly-L-lysine, fibronectin and both of them. They were photographed under microscope.

PLL was used, because it is a kind of aminoacid play role in adhesion. Fibronectin was used because it is one of the most abundant proteins in extracellular matrix. PDMS surface without coating was used as control. Experiment result showed that PLL + FN coated channels were better adhesion promoting surfaces than other group coatings (Figure 3.3). For this process, PDMS molds sticked on the glass were exposed UV for 30 minutes and channels were coated PLL with 20 minutes incubation. After that PLL solution was aspirated with vacuum and FN solution was added and incubated for 1 hr to coat. After coating was complete, FN solution was aspirated. The channels were washed with ultra pure water. 2D LOC 's were stored under vacuum until used. Two different FN concentrations (0.025 mg / ml and 0.0125mg / ml) were tested and 0.0125mg / ml was concluded as sufficient (Figure 3.4 and Figure 3.5).

Surface	Number of Cells	Incubation time
PDMS	1.5×10^6 cells / ml	3 hours
PDMS	1.5×10^6 cells / ml	6 hours
PDMS	3×10^6 cells / ml	3 hours
PDMS	3×10^6 cells / ml	6 hours
PDMS	6×10^6 cells / ml	3 hours
PDMS	6×10^6 cells / ml	6 hours
PDMS + PLL	1.5×10^6 cells / ml	3 hours
PDMS + PLL	1.5×10^6 cells / ml	6 hours
PDMS + PLL	3×10^6 cells / ml	3 hours
PDMS + PLL	3×10^6 cells / ml	6 hours
PDMS + PLL	6×10^6 cells / ml	3 hours
PDMS + PLL	6×10^6 cells / ml	6 hours
PDMS + FN	1.5×10^6 cells / ml	3 hours
PDMS + FN	1.5×10^6 cells / ml	6 hours
PDMS + FN	3×10^6 cells / ml	3 hours
PDMS + FN	3×10^6 cells / ml	6 hours
PDMS + FN	6×10^6 cells / ml	3 hours
PDMS + FN	6×10^6 cells / ml	6 hours
PDMS + PLL + FN	1.5×10^6 cells / ml	3 hours
PDMS + PLL + FN	1.5×10^6 cells / ml	6 hours
PDMS + PLL + FN	3×10^6 cells / ml	3 hours
PDMS + PLL + FN	3×10^6 cells / ml	6 hours
PDMS + PLL + FN	6×10^6 cells / ml	3 hours
PDMS + PLL + FN	6×10^6 cells / ml	6 hours

Table 3.1. Combinations tested for optimization of the surface, the numer of cells and culture time

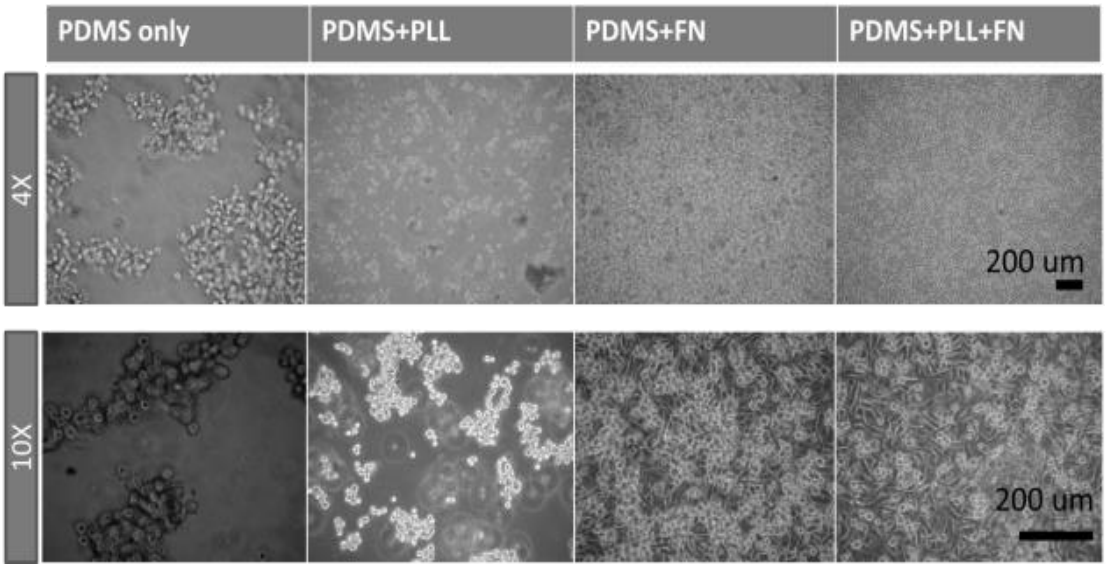

Figure 3.3. Phase contrast images of cells on PDMS, PLL coated PDMS, FN coated PDMS, PLL+FN coated PDMS with 4X ve 10X magnification.

Three different concentrations and two different culture time were tested to optimize the number of cells. As the number of cells 1.5×10^6 cells / mL, 3×10^6 cells / ml, 6×10^6 cells / ml were used while as the culture time, 3 hours and 6 hours were tested. 1.5×10^6 cells / ml for 3 and 6 hour incubation resulted adequate coating on PDMS. It would cause a decrease in the culture medium if the culture period was extended. Moreover, additional culture media from the medium reservoir could not be provided. Becasue of this longer culture period was not tried. 3×10^6 cells / ml for 6 hours incubation was enough to result in complete cell confluency into channels. 6×10^6 cells / ml of cell concentration with 3 hours and 6 hours incubation were successed in coating the surface, but in order to use minimum cell number and material, 3×10^6 cells / ml cell concentration with 6 hours incubation was decided for further experiments.

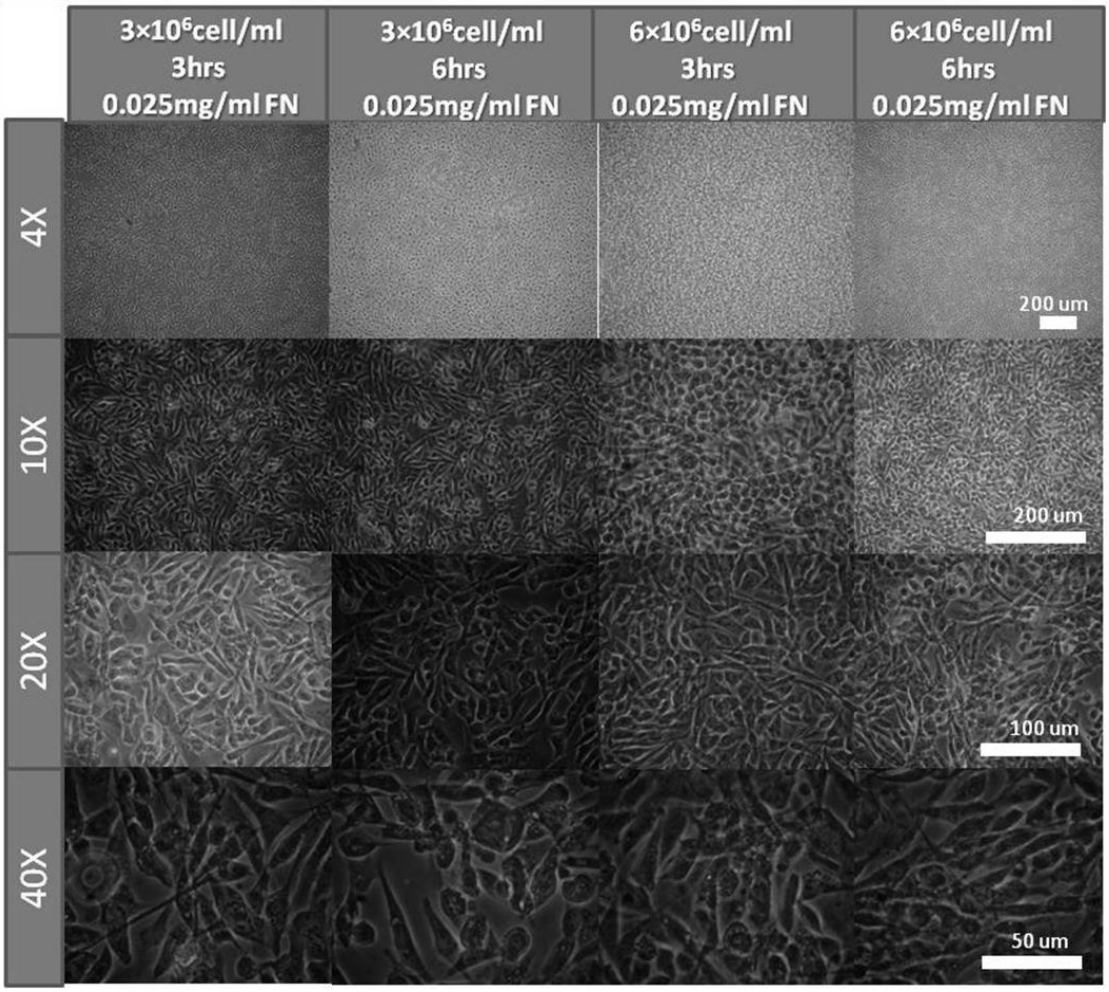

Figure 3.4. Different cell concentration seeded on PLL and 0.025 mg/ml FN coated PDMS surface with 4X, 10X, 20X, 40X magnification.

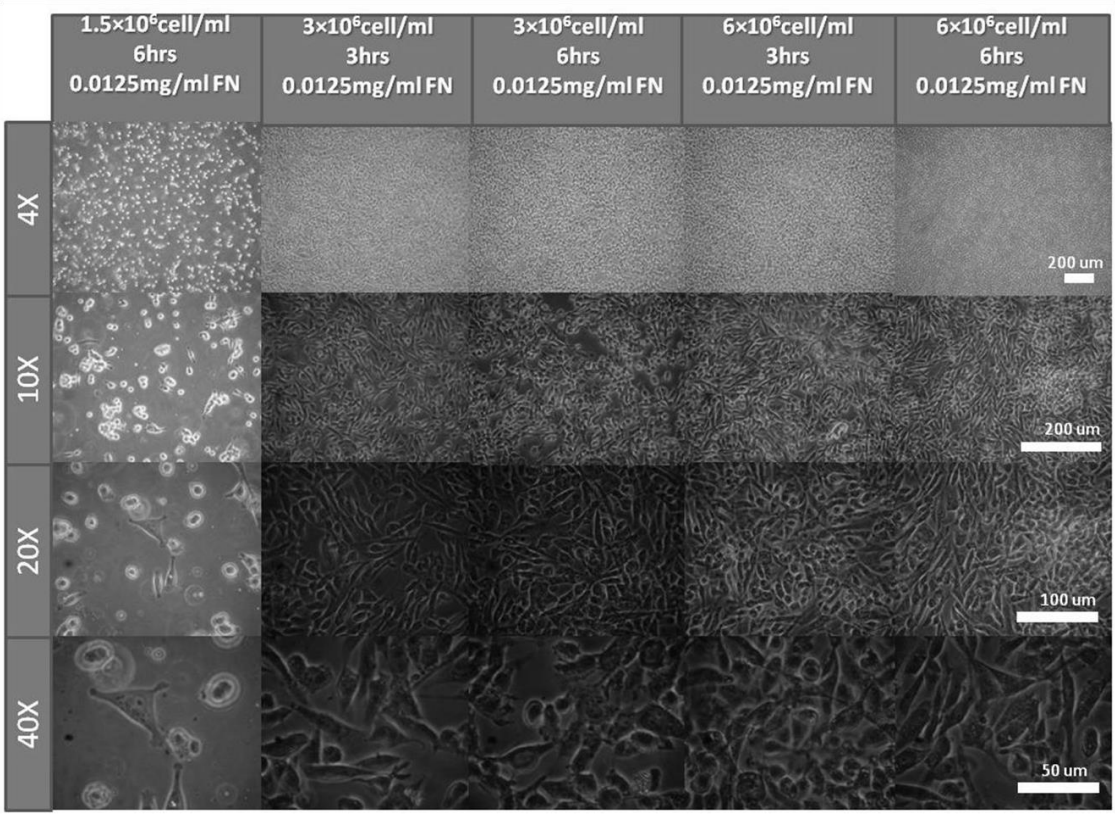

Figure 3.5. Different cell concentration seeded on PLL and 0.0125 mg/ml FN coated PDMS surface with 4X, 10X, 20X, 40X magnification.

MDA-MB-231 and MCF10A cells were inspected under microscope and images were taken under decided condition (PLL + FN coated PDMS surface; 3×10^6 cells / mL and 6 hours of incubation). It was observed that both cell lines lived long time and seen healthy in LOC.

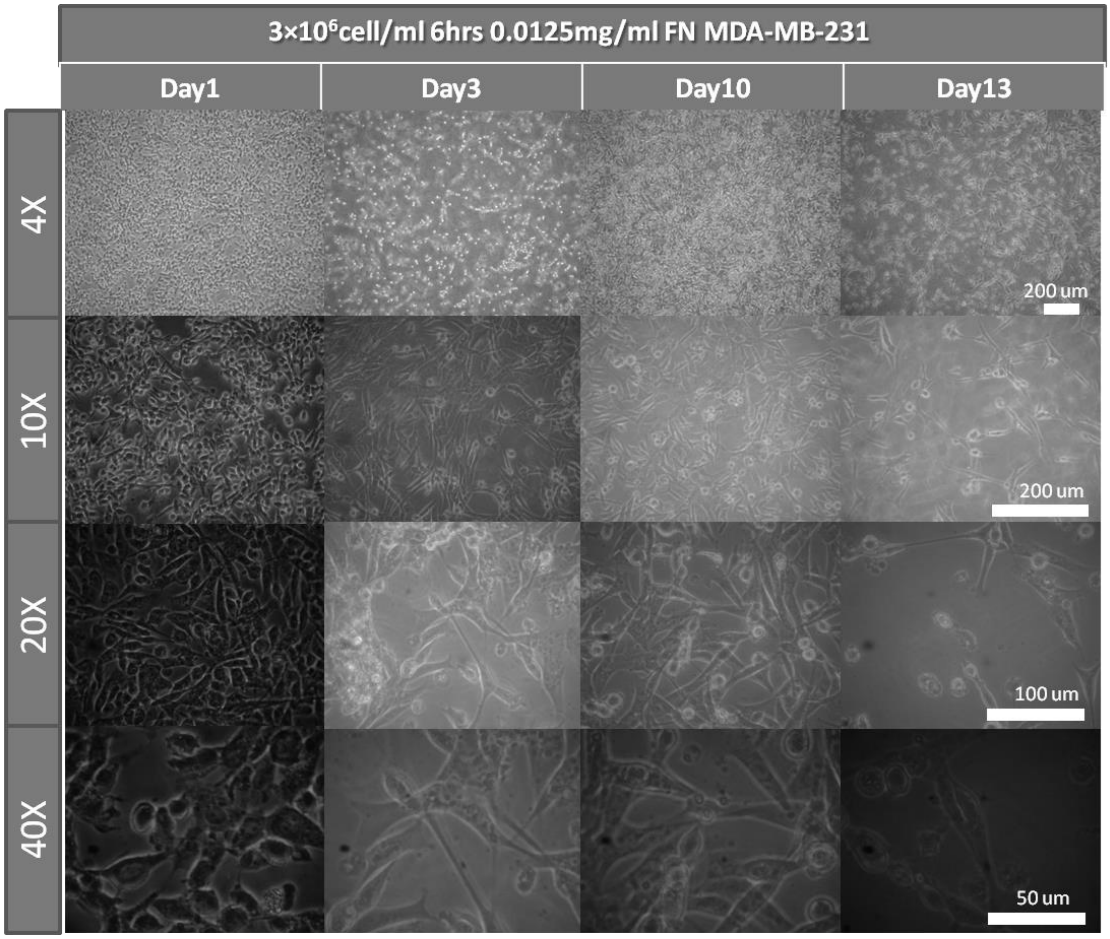

Figure 3.6. MDA-MB-231 cells on different days, seeded on PLL+FN coated PDMS surface at 3 × 106 cells / ml concentration and incubated for 6 hours. Images were taken with 4X, 10X, 20X, 40X objectives.

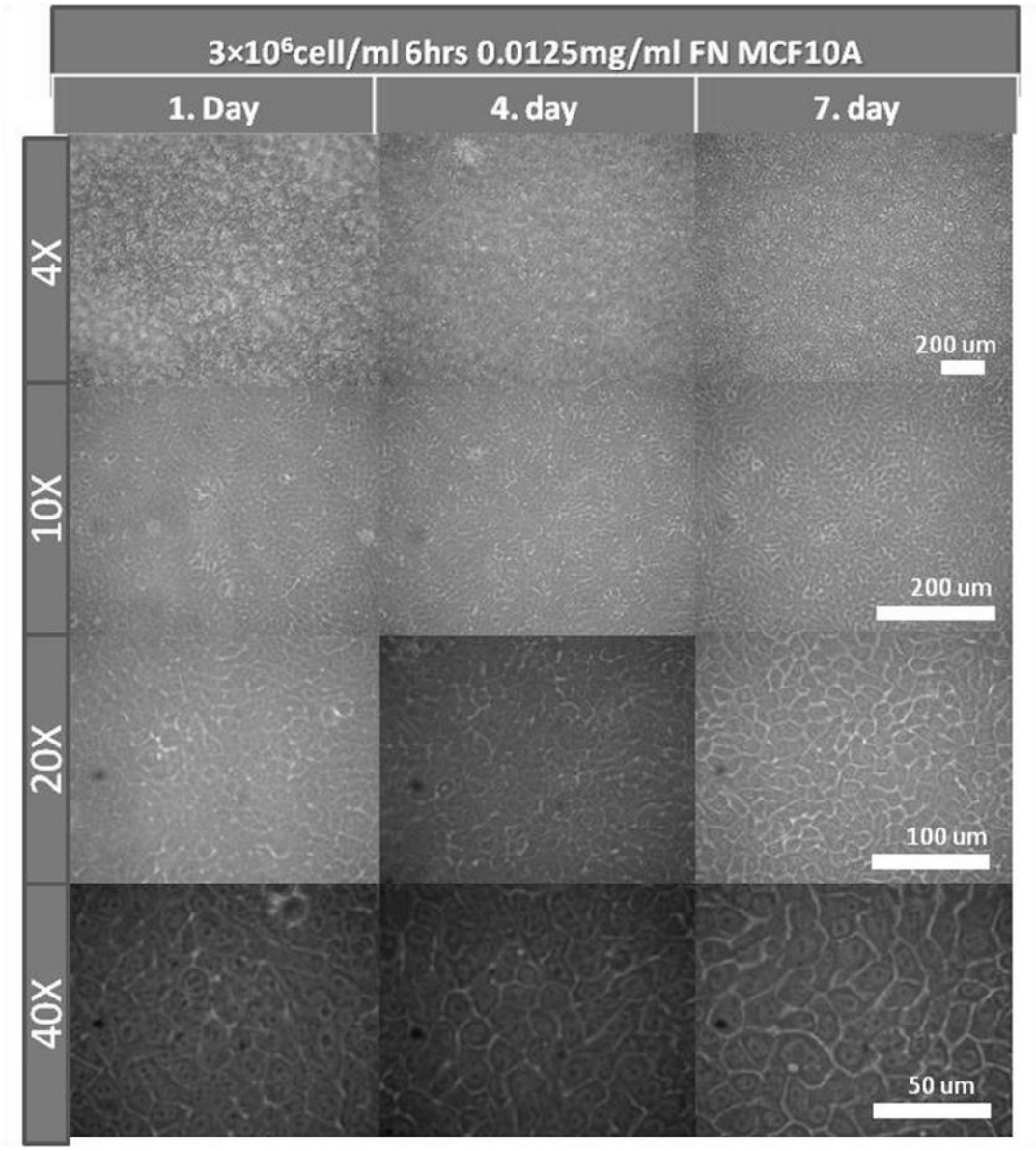

Figure 3.7. MCF10A cells on different days, seeded on PLL+FN coated PDMS surface at 3×10^6 cells / ml concentration and incubated for 6 hours. Images were taken with 4X, 10X, 20X, 40X objectives.

3.4. Co-Culture Medium Trials

Due to the co-culture experiments of MDA-MB-231 and MCF10A in LOC system, experiments were carried out in order to find medium that both cell lines could grow. In order to optimize these in 3D system, matrigel and cells were mixed as 1:1 ratio and loaded as drop on petri dish surface. Petri dish was hold as upside down and matrigel was allowed to polymerize in half an hour. Then, different culture mediums were added to petri dishes and matrigel drops were observed for cell growth and proliferation up to 10 days.

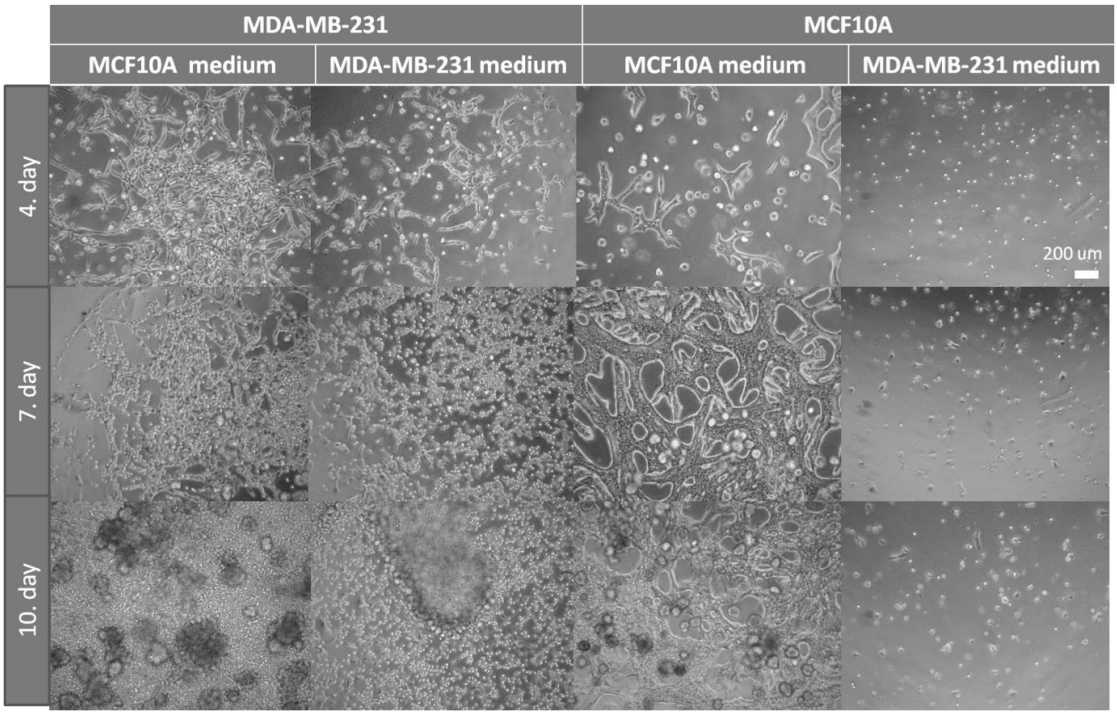

Figure 3.8. MCF10A and MDA-MB-231 cell images in MCF10A and MDA-MB-231 medium.

MCF10A cells in MDA-MB-231 medium did not show the normal course of growth and proliferation, however, MDA-MB-231 cells in MCF10A medium showed ordinary course of growth and proliferation. Based on these results, MCF10A medium was decided to use as the culture medium in co-culture experiments. Images were taken using the 4X objective.

3.5. Analysis the Effect of Doxorubicin on 2D Cultured Cells in 24 well plate

24 well plates are popular materials to determine the effects of drugs. For this purpose, metastatic breast cancer cells (MDA-MB-231 cells) and normal mammary epithelial cells (MCF10A cells) were seeded at 200,000 cells/ well concentration to 24 well plate and incubated for 48 hours at 37°C, 5% CO_2. After the incubation, pre-determined doxorubicin concentrations [0.5 µM, 1.5 µM, 2.5 µM, 5 µM and 10 µM] and doxorubicin free medium were applied to cells. Afterwards cells were observed under phase-contrast and florescence microscopes at 555 nm wavelength, with 40X lens at 24, 48 and 72 hours for visualizing the entrance of the drug into the cells.

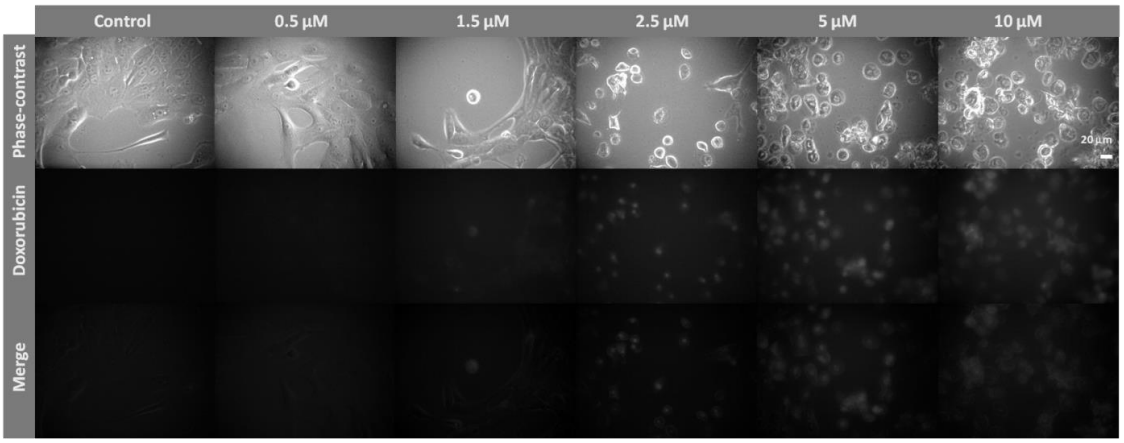

Figure 3.9. Phase-contrast and fluorescent images of MCF10A cells in 2D 24 well plate at the concentration of 200,000 cells/well under the exposure of varying concentrations of doxorubicin at 24 hrs. Scale is 20 µm.

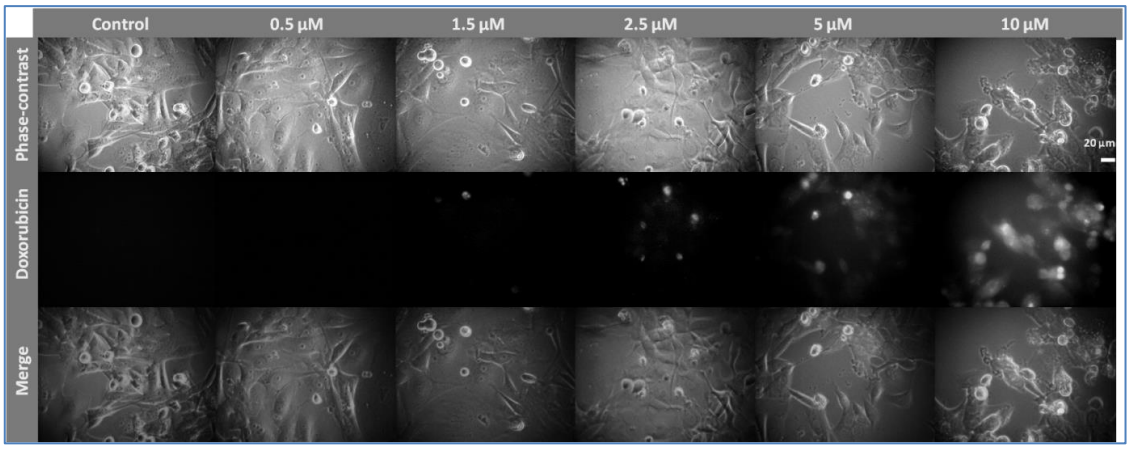

Figure 3.10. Phase-contrast and fluorescent images of MDA-MB-231 cells in 2D 24 well plate at the concentration of 200,000 cells/well under the exposure of varying concentrations of doxorubicin at 24 hrs. Scale is 20 µm.

Figure 3.9 and Figure 3.10 show phase-contrast, doxorubicin and merge images of MCF10A and MDA-MB-231 cells in 24-well system. Drug was introduced into the cell at 0.5 µM concentration and it was observed that fluorescence signal increased with increasing drug concentration. Increased drug concentration has led to deterioration in the morphology of the cells.

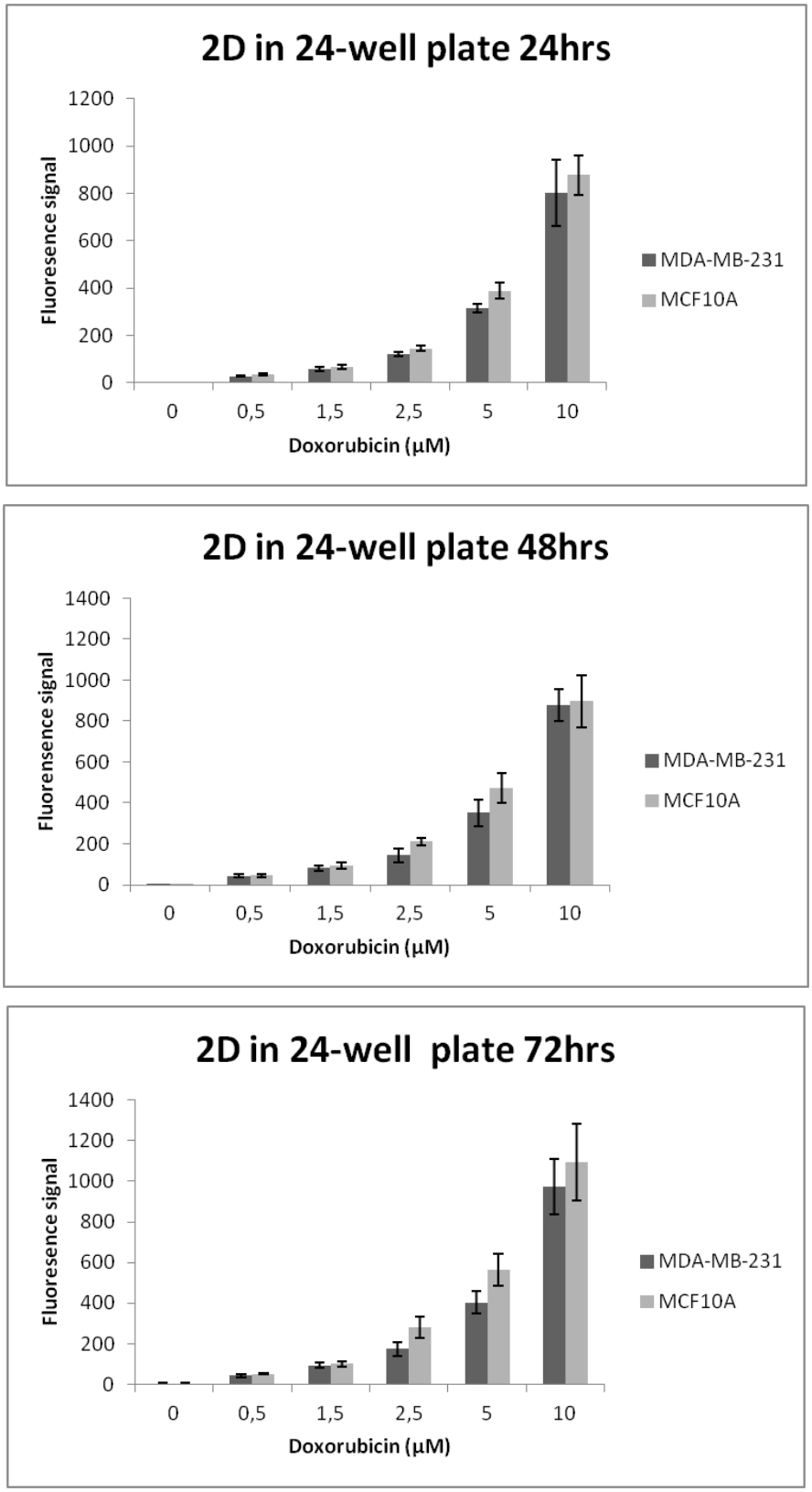

Figure 3.11. Fluorescence signals of MDA-MB-231 and MCF10A cells in 2D 24 well plate at 24, 48 and 72 hours respectively.

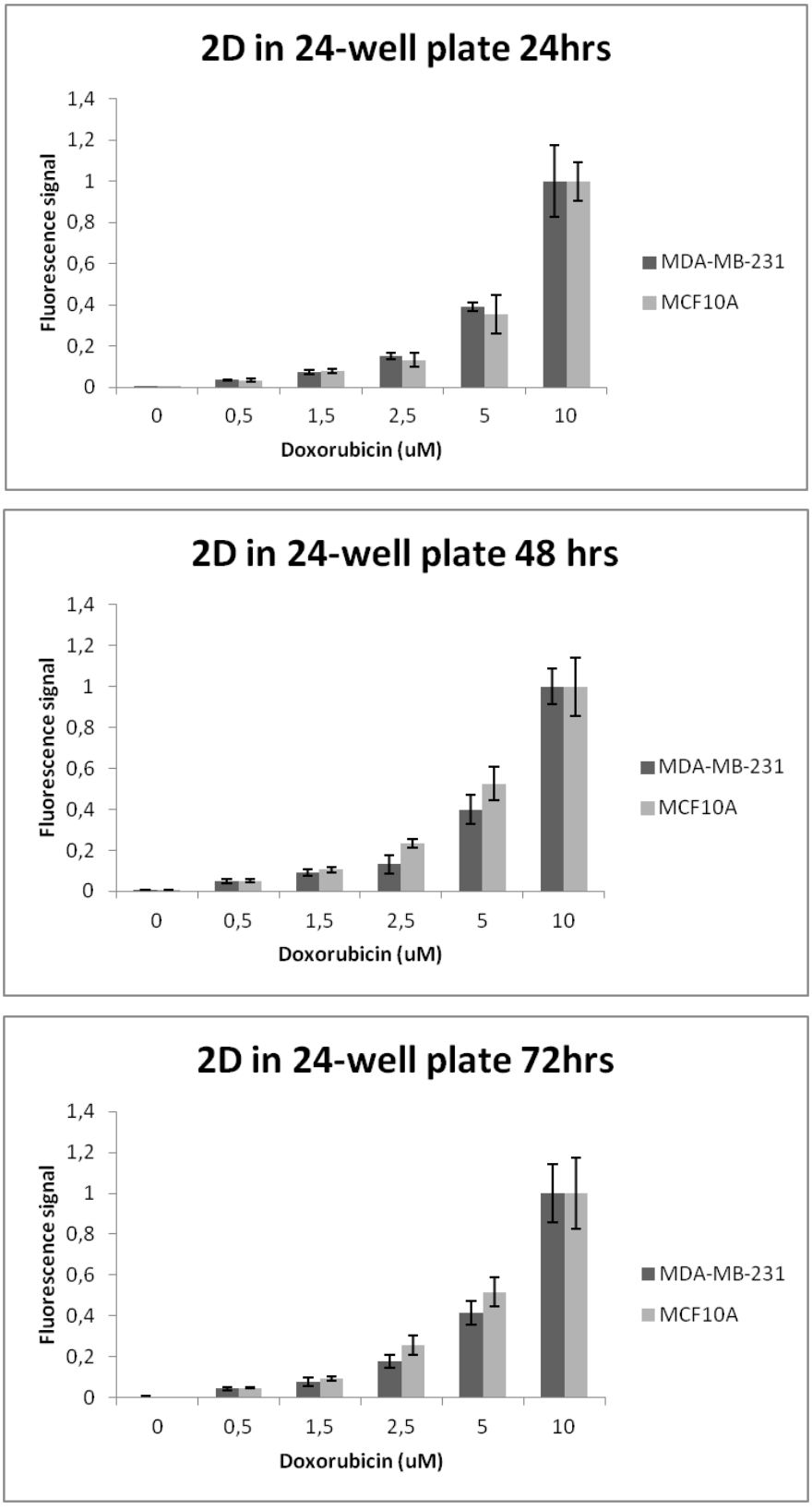

Figure 3.12. Normalized to highest fluorescence signals of each group

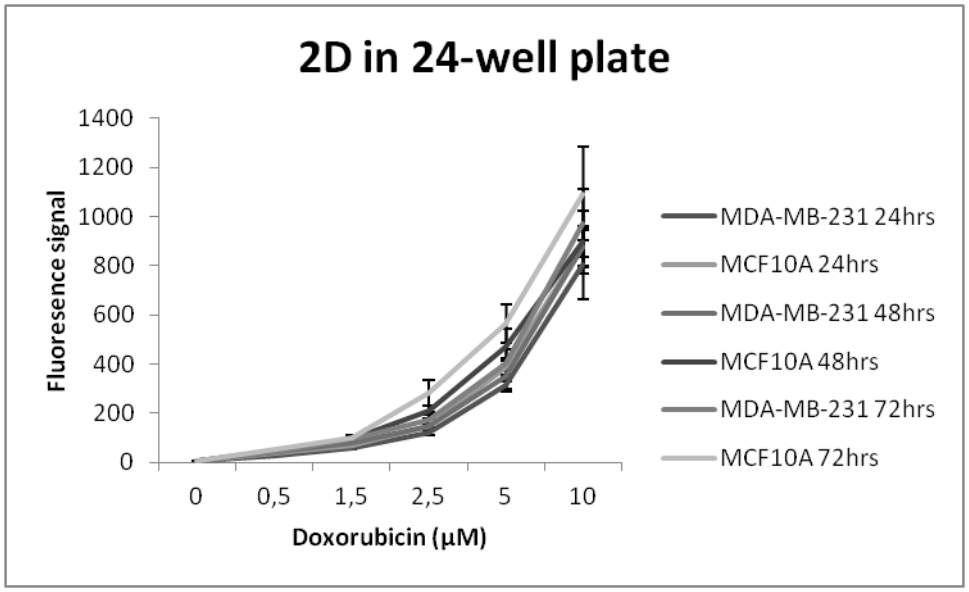

Figure 3.13. Fluorescence signals MDA-MB-231 and MCF10A cells in 2D 24 well plate with variation of time and concentration of doxorubicin.

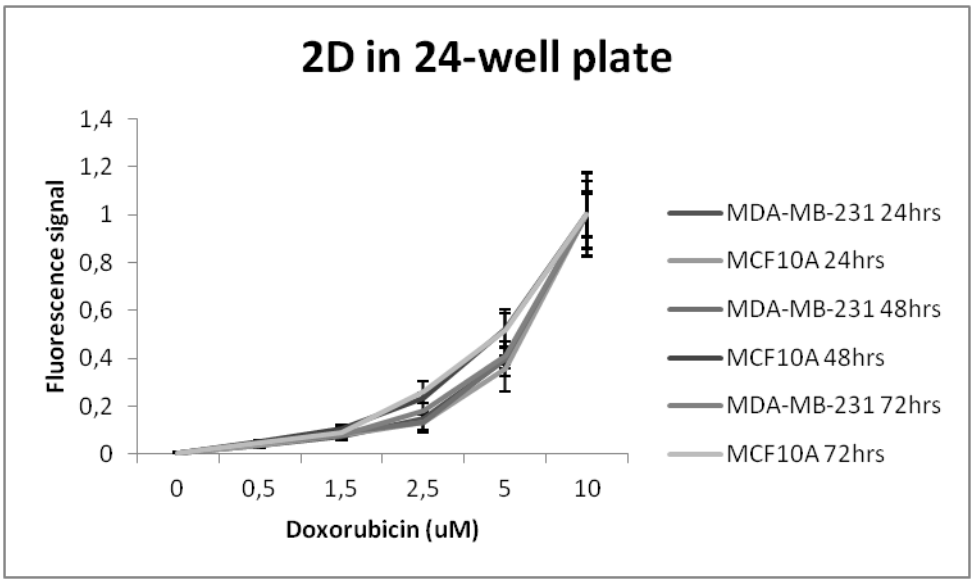

Figure 3.14. Normalized to highest fluorescence signals of each group

MCF10A 24h 2D 24well	0 uM	0,5 uM	1,5 uM	2,5 uM	5 uM	10 uM
0 uM	1	0,008590441	0,001264087	0,001127756	0,00124135	0,000465964
0,5 uM	0,008590441	1	0,013909492	0,000981149	0,001678191	0,000545241
1,5 uM	0,001264087	0,013909492	1	0,001343966	0,002292147	0,000635258
2,5 uM	0,001127756	0,000981149	0,001343966	1	0,001983661	0,000952357
5 uM	0,00124135	0,001678191	0,002292147	0,001983661	1	0,002783133
10 uM	0,000465964	0,000545241	0,000635258	0,000952357	0,002783133	1

MDA-MB-231 24h 2D 24well	0 uM	0,5 uM	1,5 uM	2,5 uM	5 uM	10 uM
0 uM	1	0,000111919	0,003593596	0,000428593	4,99892E-05	0,004737004
0,5 uM	0,000111919	1	0,017101209	0,00104726	6,92071E-05	0,005267625
1,5 uM	0,003593596	0,017101209	1	0,00220212	1,01075E-05	0,006176046
2,5 uM	0,000428593	0,00104726	0,00220212	1	2,50842E-05	0,008427173
5 uM	4,99892E-05	6,92071E-05	1,01075E-05	2,50842E-05	1	0,026168881
10 uM	0,004737004	0,005267625	0,006176046	0,008427173	0,026168881	1

MCF10A 48h 2D 24well	0 uM	0,5 uM	1,5 uM	2,5 uM	5 uM	10 uM
0 uM	1	0,006634249	0,002813741	0,000384113	0,002905919	0,00218363
0,5 uM	0,006634249	1	0,022259291	0,00045748	0,004180263	0,002626707
1,5 uM	0,002813741	0,022259291	1	0,00149598	0,006742229	0,003311111
2,5 uM	0,000384113	0,00045748	0,00149598	1	0,017251872	0,005983595
5 uM	0,002905919	0,004180263	0,006742229	0,017251872	1	0,027191132
10 uM	0,00218363	0,002626707	0,003311111	0,005983595	0,027191132	1

MDA-MB-231 48h 2D 24well	0 uM	0,5 uM	1,5 uM	2,5 uM	5 uM	10 uM
0 uM	1	0,007101	0,006218761	0,02581034	0,005702642	0,000361138
0,5 uM	0,007101	1	0,05878911	0,061605794	0,008900377	0,000438756
1,5 uM	0,006218761	0,05878911	1	0,161666799	0,01493793	0,000552595
2,5 uM	0,02581034	0,061605794	0,161666799	1	0,029787818	0,000347283
5 uM	0,005702642	0,008900377	0,01493793	0,029787818	1	0,000802861
10 uM	0,000361138	0,000438756	0,000552595	0,000347283	0,000802861	1

MCF10A 72h 2D 24well	0 uM	0,5 uM	1,5 uM	2,5 uM	5 uM	10 uM
0 uM	1	2,83072E-05	0,001216738	0,005978737	0,00201478	0,004534729
0,5 uM	2,83072E-05	1	0,010364637	0,011590786	0,00280944	0,005331588
1,5 uM	0,001216738	0,010364637	1	0,026921458	0,00418676	0,006357484
2,5 uM	0,005978737	0,011590786	0,026921458	1	0,01971777	0,009105993
5 uM	0,00201478	0,00280944	0,00418676	0,01971777	1	0,049844903
10 uM	0,004534729	0,005331588	0,006357484	0,009105993	0,049844903	1

MDA-MB-231 72h 2D 24well	0 uM	0,5 uM	1,5 uM	2,5 uM	5 uM	10 uM
0 uM	1	0,003982069	0,005792845	0,00655782	0,002105142	0,002134457
0,5 uM	0,003982069	1	0,016779183	0,017263562	0,003162059	0,002495082
1,5 uM	0,005792845	0,016779183	1	0,070818951	0,005830999	0,003103989
2,5 uM	0,00655782	0,017263562	0,070818951	1	0,01231385	0,004776326
5 uM	0,002105142	0,003162059	0,005830999	0,01231385	1	0,012025099
10 uM	0,002134457	0,002495082	0,003103989	0,004776326	0,012025099	1

Table 3.2. T-test values for MCF10A and MDA-MB-231 cells between different doses at 24, 48 and 72 hours respectively. Dark values indicate significant differences ($p<0.05$ two tail level).

MCF10A 2D 24well	0 uM	0.5 uM	1.5 uM	2.5 uM	5 uM	10 uM
24-48 hrs	0,960679211	0,404746207	0,145662873	0,023382827	0,343618585	0,898133031
48-72 hrs	0,745025184	0,482141571	0,745081486	0,253374159	0,402332955	0,417916496
24-72 hrs	0,734872736	0,057804018	0,053725019	0,061443818	0,09146259	0,34283535

MDA-MB-231 2D 24well	0 uM	0.5 uM	1.5 uM	2.5 uM	5 uM	10 uM
24-48 hrs	0,809041013	0,112155558	0,248902096	0,161666799	0,613302334	0,651346715
48-72 hrs	0,550522551	0,924375818	0,506763973	0,555763974	0,562206377	0,5730361
24-72 hrs	0,722434443	0,086516016	0,06176777	0,184609959	0,195663098	0,410617501

Table 3.3. T-test values for MCF10A and MDA-MB-231 cells between different time points. Dark values indicate significant differences ($p<0.05$ two tail level)

MCF10A vs. MDA-MD-231 2D 24well	0 uM	0.5 uM	1.5 uM	2.5 uM	5 uM	10 uM
24 hrs	0,821055146	0,173917959	0,518740117	0,175756538	0,096078123	0,666918492
48 hrs	0,943357724	0,813992096	0,540320124	0,149406774	0,246891728	0,909402042
72 hrs	0,70918268	0,352178369	0,757215863	0,11993824	0,134271325	0,62382188

Table 3.4. T-test values between MCF10A and MDA-MB-231 cells at different time points.

According to the analysis performed, it was observed that fluorescence signal has increased as the concentration of the drug increased in 24 well system. Yet, no significant difference in drug uptake between two cell lines (MCF10A and MDA-MB-231) was observed. According to the images taken at 24, 48 and 72 hours, no significant increase in drug uptake in 24 well plate is observed after 24 hours with the correlation of time. This has shown that, in this system drug was taken within the cell within 24 hours predominantly.

3.6. Analysis of Effect of Doxorubicin on 2D Cultured Cells on Chip

Drug dosages were applied to cells using 2D chips that have been previously optimized. Chips were coated with poly-L-lysine and fibronectin after PDMS mold preparation, cleaning, and channel preparation using glass. MDA-MB-231 and MCF10A cells were seeded on chips at $3x10^6$ cells / ml. After incubation, varying concentrations [0, 0.5µM, 1.5µM, 2.5µM, 5µM, 10µM] of doxorubicin were administered to cells. After drug administration, pictures of the cells were taken at 24, 48, and 72 hours and analyzed. Drawings obtained from the phase-contrast pictures microscopy were applied to doxorubicin pictures and the amount of drug taken by the cells was evaluated using fluorescence intensity.

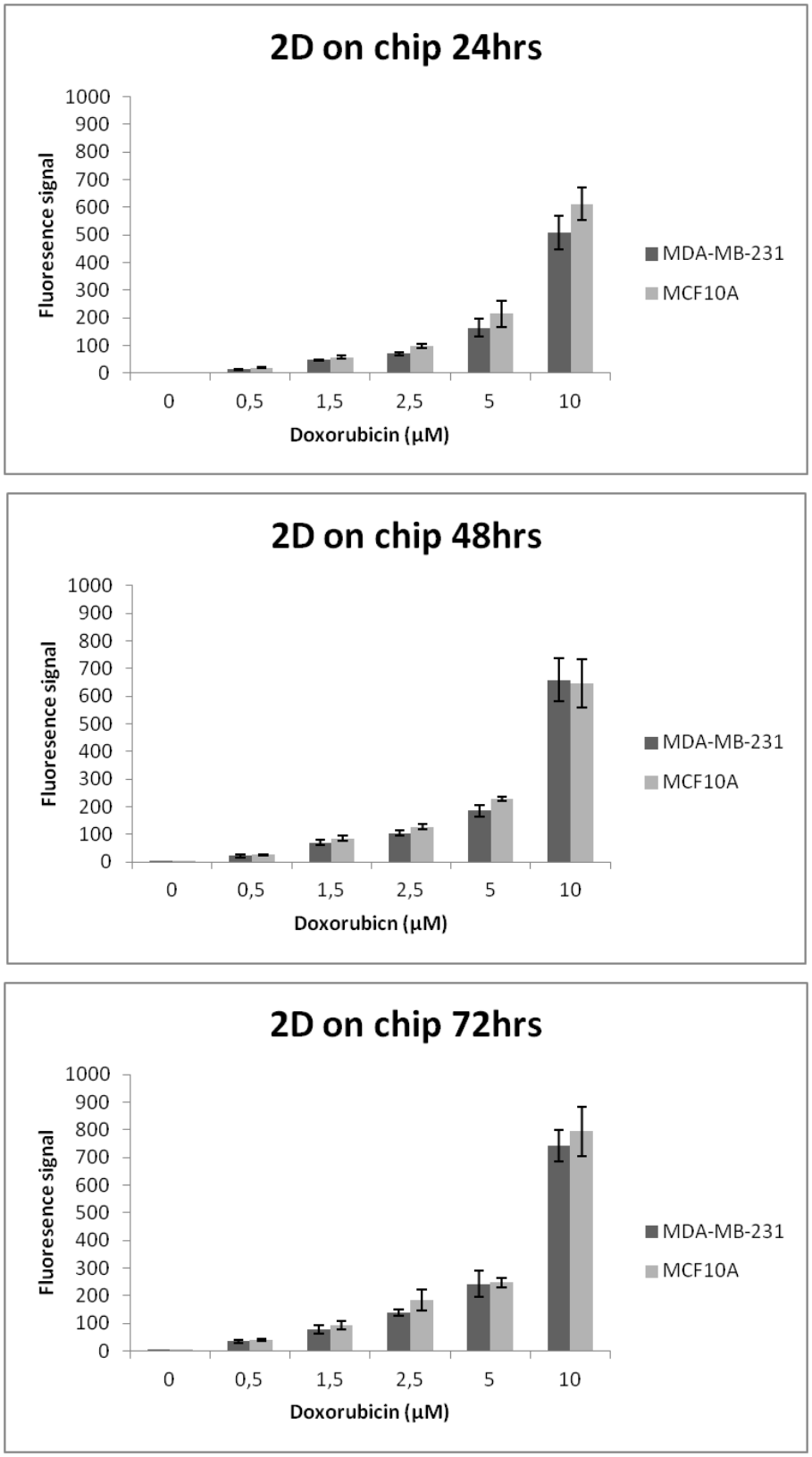

Figure 3.15. Fluorescence signals of MDA-MB-231 and MCF10A cells in 2D LOC system at 24, 48 and 72 hours respectively.

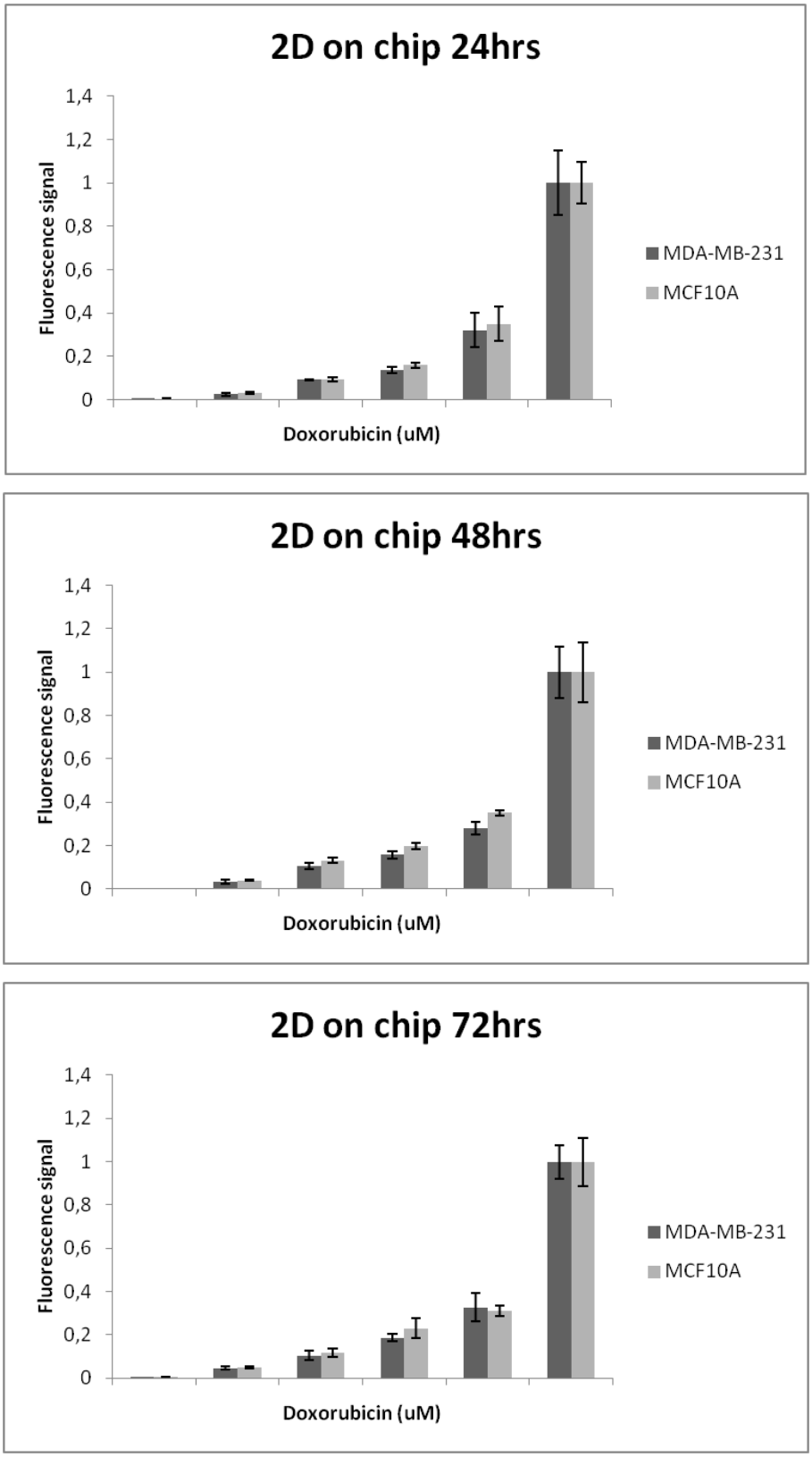

Figure 3.16. Normalized to highest fluorescence signals of each group

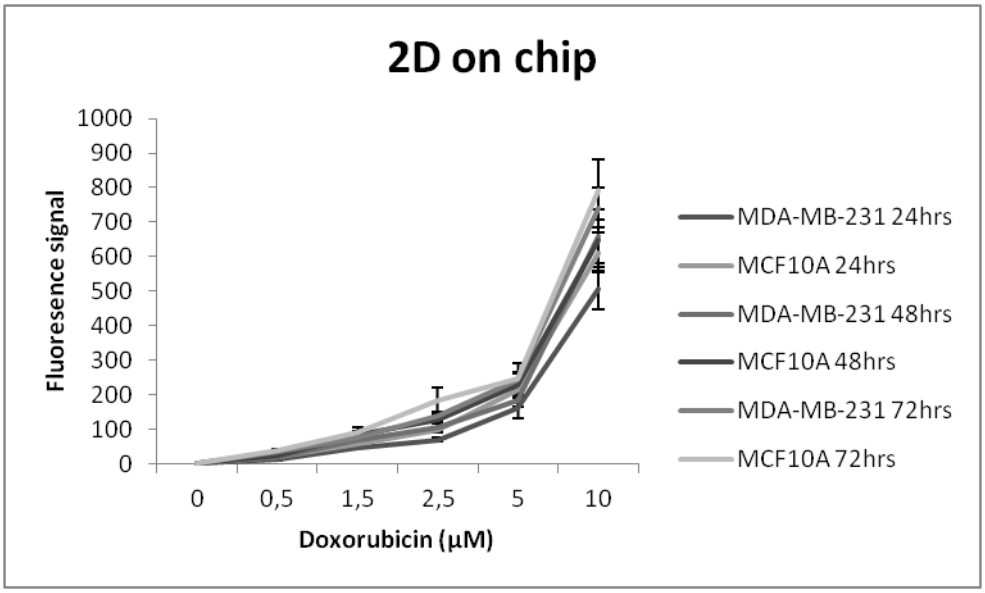

Figure 3.17. Fluorescence signals of MDA-MB-231 and MCF10A cells in 2D LOC system with variation of time and concentration of doxorubicin

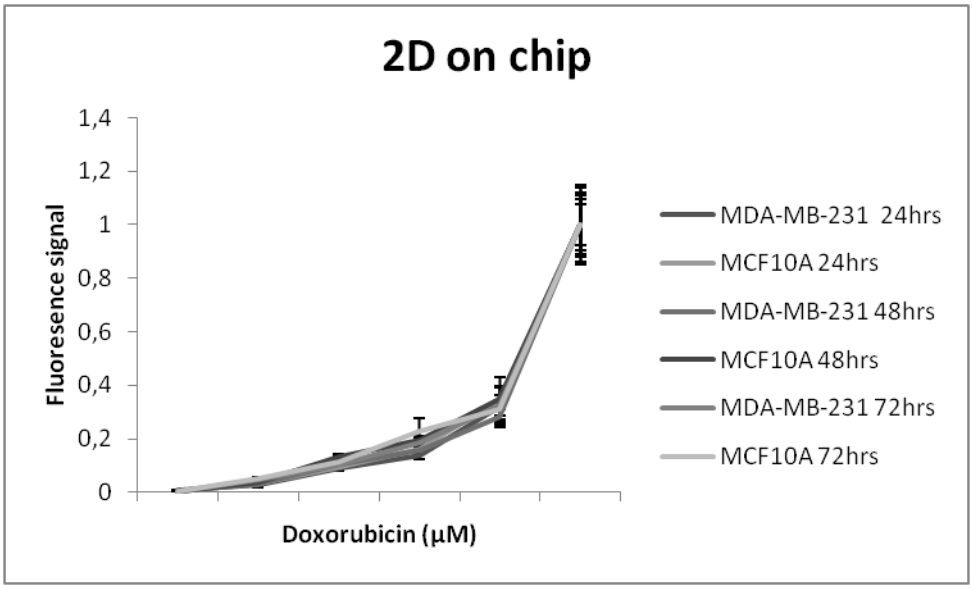

Figure 3.18. Normalized to highest fluorescence signals of each group

MCF10A 24h 2D CHIP	0 uM	0,5 uM	1,5 uM	2,5 uM	5 uM	10 uM
0 uM	1	0,004847728	0,000444062	0,000222534	0,022738472	0,000462415
0,5 uM	0,004847728	1	0,000719578	0,000199283	0,028602901	0,000519585
1,5 uM	0,000444062	0,000719578	1	0,002929985	0,049781585	0,000676659
2,5 uM	0,000222534	0,000199283	0,002929985	1	0,100349706	0,000921743
5 uM	0,022738472	0,028602901	0,049781585	0,100349706	1	0,001195131
10 uM	0,000462415	0,000519585	0,000676659	0,000921743	0,001195131	1

MDA-MB-231 24h 2D CHIP	0 uM	0,5 uM	1,5 uM	2,5 uM	5 uM	10 uM
0 uM	1	0,053284647	1,6274E-05	0,000754676	0,015601273	0,002580166
0,5 uM	0,053284647	1	0,000140602	0,000386863	0,019431988	0,002784339
1,5 uM	1,6274E-05	0,000140602	1	0,034543913	0,042629266	0,003608703
2,5 uM	0,000754676	0,000386863	0,034543913	1	0,082397756	0,004437509
5 uM	0,015601273	0,019431988	0,042629266	0,082397756	1	0,006679342
10 uM	0,002580166	0,002784339	0,003608703	0,004437509	0,006679342	1

MCF10A 48h 2D CHIP	0 uM	0,5 uM	1,5 uM	2,5 uM	5 uM	10 uM
0 uM	1	0,00059386	0,000550861	0,000223986	1,06624E-05	0,001898208
0,5 uM	0,00059386	1	0,000896801	0,000542348	2,48967E-06	0,002174544
1,5 uM	0,000550861	0,000896801	1	0,011480824	1,86545E-06	0,003216953
2,5 uM	0,000223986	0,000542348	0,011480824	1	5,1174E-05	0,0042992
5 uM	1,06624E-05	2,48967E-06	1,86545E-06	5,1174E-05	1	0,009161739
10 uM	0,001898208	0,002174544	0,003216953	0,0042992	0,009161739	1

MDA-MB-231 48h 2D CHIP	0 uM	0,5 uM	1,5 uM	2,5 uM	5 uM	10 uM
0 uM	1	0,022393997	0,001749867	0,000795128	0,000741807	0,001106274
0,5 uM	0,022393997	1	0,003592862	0,000510649	0,000473713	0,001246273
1,5 uM	0,001749867	0,003592862	1	0,039423836	0,001731081	0,001704338
2,5 uM	0,000795128	0,000510649	0,039423836	1	0,011936649	0,002176768
5 uM	0,000741807	0,000473713	0,001731081	0,011936649	1	0,004181746
10 uM	0,001106274	0,001246273	0,001704338	0,002176768	0,004181746	1

MCF10A 72h 2D CHIP	0 uM	0,5 uM	1,5 uM	2,5 uM	5 uM	10 uM
0 uM	1	0,000147299	0,004089542	0,008814454	0,000166448	0,000870883
0,5 uM	0,000147299	1	0,026807501	0,019319155	0,0003281	0,001047524
1,5 uM	0,004089542	0,026807501	1	0,075285178	0,000161615	0,001451259
2,5 uM	0,008814454	0,019319155	0,075285178	1	0,173344374	0,001436358
5 uM	0,000166448	0,0003281	0,000161615	0,173344374	1	0,003777597
10 uM	0,000870883	0,001047524	0,001451259	0,001436358	0,003777597	1

MDA-MB-231 72h 2D CHIP	0 uM	0,5 uM	1,5 uM	2,5 uM	5 uM	10 uM
0 uM	1	0,00973979	0,010375271	0,000496585	0,008207824	0,000211221
0,5 uM	0,00973979	1	0,057823295	0,000384972	0,013569761	0,000255634
1,5 uM	0,010375271	0,057823295	1	0,017723439	0,023570419	0,000100868
2,5 uM	0,000496585	0,000384972	0,017723439	1	0,094498581	0,000509807
5 uM	0,008207824	0,013569761	0,023570419	0,094498581	1	0,000166731
10 uM	0,000211221	0,000255634	0,000100868	0,000509807	0,000166731	1

Table 3.5. T-test values for MCF10A and MDA-MB-231 cells between different doses at 24, 48 and 72 hours respectively. Dark values indicate significant differences ($p<0.05$ two tail level).

MCF10A 2D CHIP	0 uM	0.5 uM	1.5 uM	2.5 uM	5 uM	10 uM
24-48 hrs	0,743689891	0,175451886	0,023743534	0,05123151	0,815161753	0,751660703
48-72 hrs	0,713270658	0,003488498	0,722180277	0,21261576	0,343980129	0,273917394
24-72 hrs	0,9978483	0,001069217	0,084198583	0,092597722	0,562260324	0,12941636

MDA-MB-231 2D CHIP	0 uM	0.5 uM	1.5 uM	2.5 uM	5 uM	10 uM
24-48 hrs	0,643869435	0,200545693	0,067327711	0,035946827	0,642877763	0,206135963
48-72 hrs	0,174041117	0,174408874	0,067327711	0,324879579	0,324879579	0,420740448
24-72 hrs	0,254456668	0,028914398	0,138278941	0,003922835	0,244655511	0,04401874

Table 3.6. T-test values for MCF10A and MDA-MB-231 cells between different time points. Dark values indicate significant differences ($p<0.05$ two tail level)

MCF10A vs. MDA-MD-231 2D CHIP	0uM	0.5 uM	1.5 uM	2.5 uM	5 uM	10 uM
24 hrs	0,335864834	0,178086334	0,108899276	0,44706776	0,211385738	0,30828963
48 hrs	0,60150304	0,546443319	0,233110141	0,171476119	0,1020337	0,927731402
72 hrs	0,101684091	0,494661376	0,512085563	0,312859585	0,926525735	0,629220119

Table 3.7. T-test values between MCF10A and MDA-MB-231 cells at different time points

Analyses showed that fluorescence signals increased with increasing doses except between 2.5 µM – 5 µM at 24 hours, 1.5 µM – 2.5 µM and 2.5 µM and 5 µM at 72 hours for MCF10A cells and between 0 µM – 0.5 µM, 2.5 µM – 5 µM at 24 hours, 0.5 µM – 1.5 µM, 1.5 µM – 2.5 µM, 2.5 µM – 5 µM at 72 hours for MDA-MB-231 cells. Significant increase was not observed with variation of time for almost all doses. According to t-test results, no significant difference in drug uptake was observed between MCF10A and MDA-MB-231 cells.

3.7. Analysis of Effect of Doxorubicin in 3D Cultured Cells in 24 well plate

To form 3D microenvironment, firstly 24 well plate system was used. $6x10^6$ cells / ml cell concentration was diluted with matrigel 1:1 ratio and cells were seeded in 24 well plate. 30 minutes later MCF10A medium was added to the cells. After two days incubation of cell-matrigel mixture, different drug concentrations [0 µM, 0.5 µM, 1.5 µM, 2.5 µM, 5 µM and 10 µM] were applied to the cells. At 24, 48, 72 hours pictures were taken and analyzed. According to pictures drug uptake was compared for both cell lines at different time points.

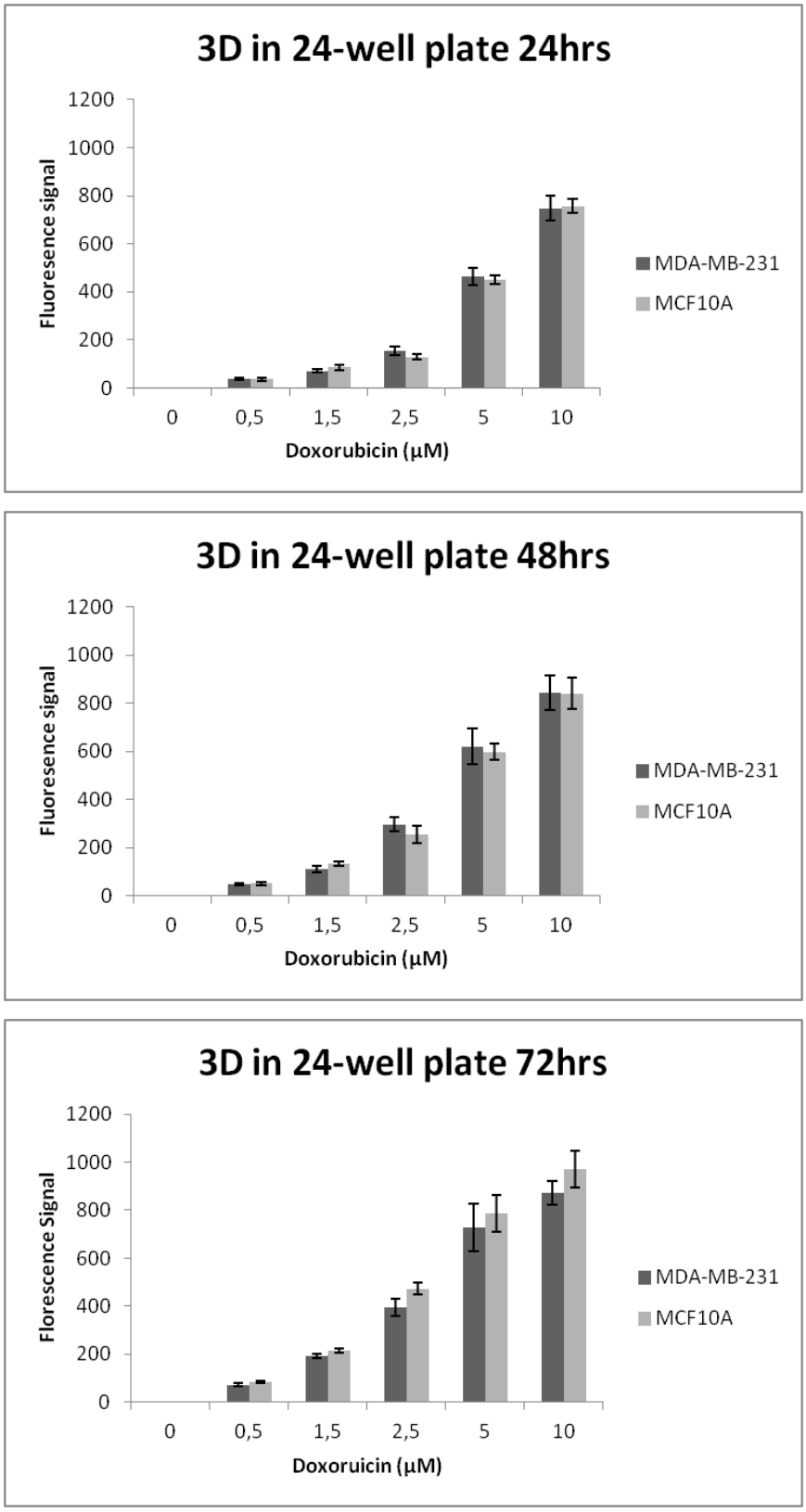

Figure 3.19. Fluorescence signals of MDA-MB-231 and MCF10A cells in 3D 24 well plate at 24, 48 and 72 hours respectively.

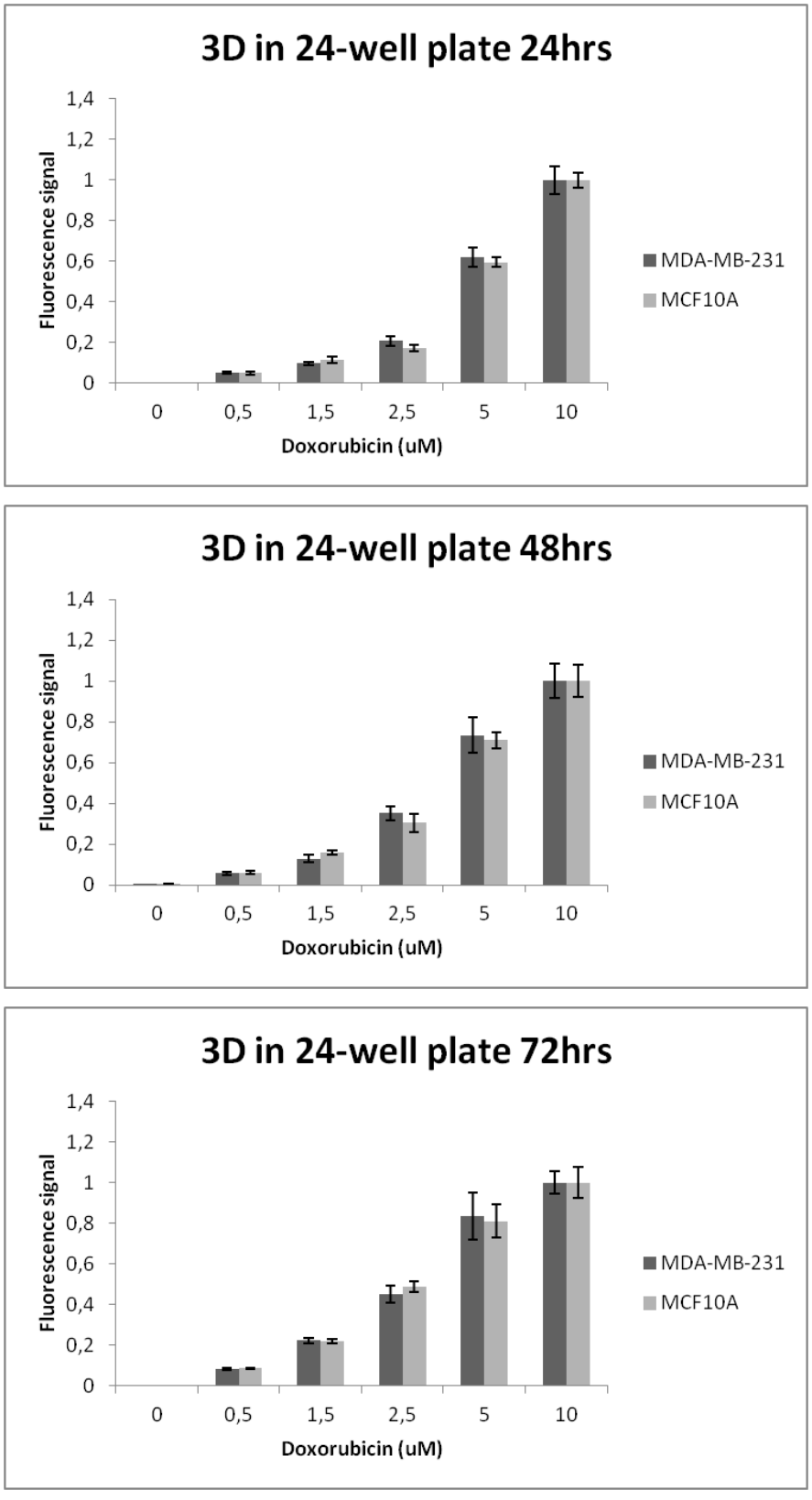

Figure 3.20. Normalized to highest fluorescence signals of each group

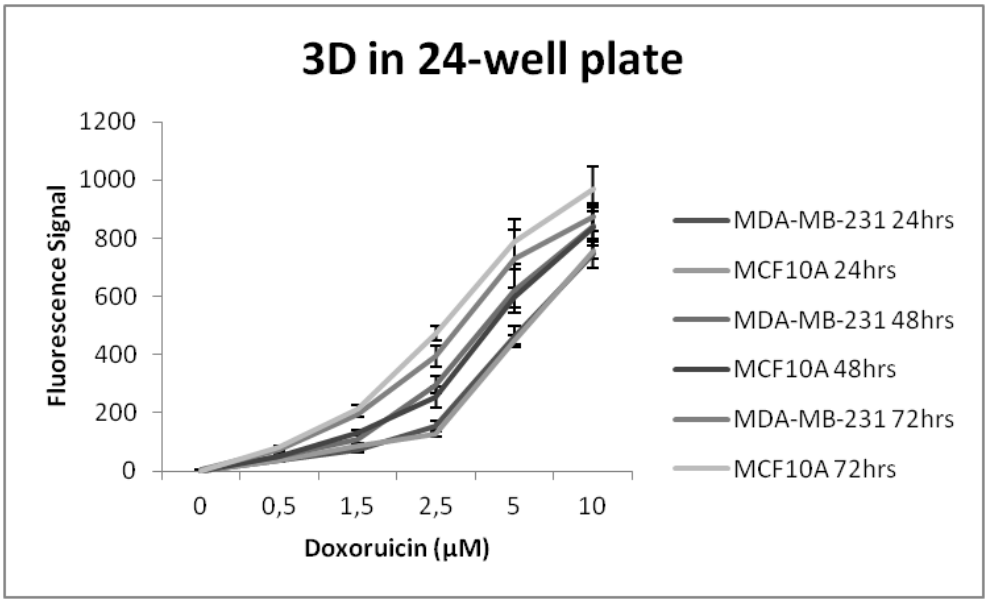

Figure 3.21. Fluorescence signals MDA-MB-231 and MCF10A cells in 3D 24 well plate with variation of time and concentration of doxorubicin

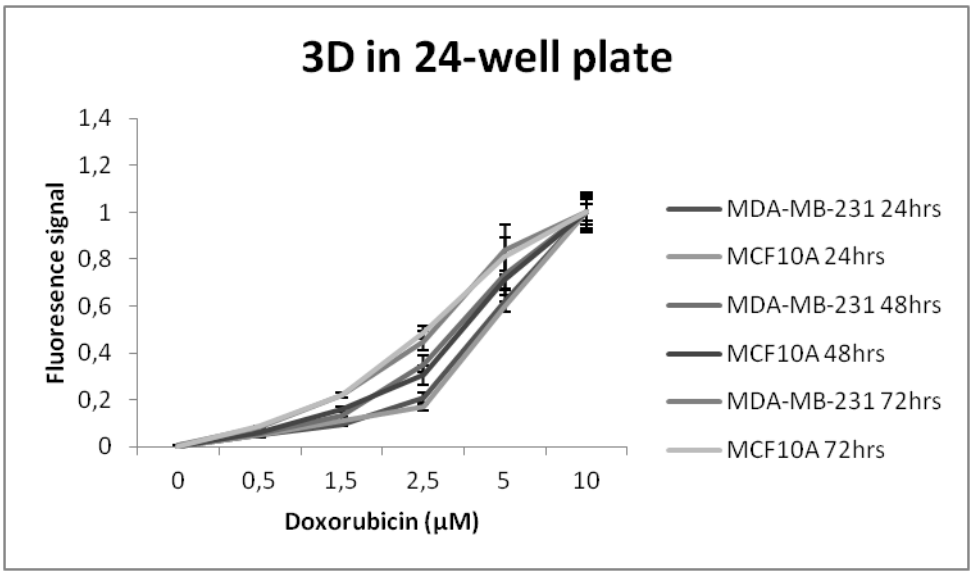

Figure 3.22. Normalized to highest fluorescence signals of each group

MCF10A 24h 3D 24well	0 uM	0.5 uM	1.5 uM	2.5 uM	5 uM	10 uM
0 uM	1	0,006149915	0,00203295	0,000106464	1,13708E-05	1,40576E-06
0,5 uM	0,006149915	1	0,011927348	0,000127312	2,88239E-06	2,90895E-07
1,5 uM	0,00203295	0,011927348	1	0,025761589	4,04387E-07	1,03926E-07
2,5 uM	0,000106464	0,000127312	0,025761589	1	9,34142E-07	1,62683E-07
5 uM	1,13708E-05	2,88239E-06	4,04387E-07	9,34142E-07	1	1,43303E-05
10 uM	1,40576E-06	2,90895E-07	1,03926E-07	1,62683E-07	1,43303E-05	1

MDA-MB-231 24h 3D 24well	0 uM	0.5 uM	1.5 uM	2.5 uM	5 Um	10 uM
0 uM	1	0,00160334	9,61322E-05	0,001046165	0,000197532	0,000696541
0,5 uM	0,00160334	1	0,001360176	0,001399657	0,000276615	0,000811072
1,5 uM	9,61322E-05	0,001360176	1	0,007102044	0,000395662	0,000950013
2,5 uM	0,001046165	0,001399657	0,007102044	1	0,000232612	0,000393132
5 uM	0,000197532	0,000276615	0,000395662	0,000232612	1	0,003764972
10 uM	0,000696541	0,000811072	0,000950013	0,000393132	0,003764972	1

MCF10A 48h 3D 24well	0 uM	0.5 uM	1.5 uM	2.5 uM	5 Um	10 uM
0 uM	1	0,003410893	0,000138732	0,000941475	0,000382319	5,04227E-05
0,5 uM	0,003410893	1	0,000119779	0,00268226	0,000531054	6,95501E-05
1,5 uM	0,000138732	0,000119779	1	0,017443094	0,000893345	0,000120818
2,5 uM	0,000941475	0,00268226	0,017443094	1	0,000121309	5,05411E-05
5 uM	0,000382319	0,000531054	0,000893345	0,000121309	1	0,012696652
10 uM	5,04227E-05	6,95501E-05	0,000120818	5,05411E-05	0,012696652	1

MDA-MB-231 48h 3D 24well	0 uM	0.5 uM	1.5 uM	2.5 uM	5 uM	10 uM
0 uM	1	0,001146862	0,001754561	0,0001778	0,003659084	0,000281665
0,5 uM	0,001146862	1	0,01038489	0,000425096	0,004594881	0,000353476
1,5 uM	0,001754561	0,01038489	1	0,000736145	0,006647914	0,000515903
2,5 uM	0,0001778	0,000425096	0,000736145	1	0,015644175	0,000825267
5 uM	0,003659084	0,004594881	0,006647914	0,015644175	1	0,064409608
10 uM	0,000281665	0,000353476	0,000515903	0,000825267	0,064409608	1

MCF10A 72h 3D 24well	0 uM	0.5 uM	1.5 uM	2.5 uM	5 uM	10 uM
0 uM	1	7,61539E-05	3,40484E-05	7,88277E-06	0,000161879	0,000215184
0,5 uM	7,61539E-05	1	6,63806E-05	2,06918E-05	0,000274334	0,000304492
1,5 uM	3,40484E-05	6,63806E-05	1	2,90785E-05	0,000746327	0,000584273
2,5 uM	7,88277E-06	2,06918E-05	2,90785E-05	1	0,008445146	0,001550454
5 uM	0,000161879	0,000274334	0,000746327	0,008445146	1	0,125361549
10 uM	0,000215184	0,000304492	0,000584273	0,001550454	0,125361549	1

MDA-MB-231 72h 3D 24well	0 uM	0.5 uM	1.5 uM	2.5 uM	5 uM	10 uM
0 uM	1	0,000282064	3,42403E-05	0,000119607	0,000760617	5,53712E-05
0,5 uM	0,000282064	1	1,08961E-05	0,000321796	0,001213015	7,89913E-05
1,5 uM	3,42403E-05	1,08961E-05	1	0,00176554	0,003063253	0,000158241
2,5 uM	0,000119607	0,000321796	0,00176554	1	0,019476941	4,59209E-05
5 uM	0,000760617	0,001213015	0,003063253	0,019476941	1	0,235034839
10 uM	5,53712E-05	7,89913E-05	0,000158241	4,59209E-05	0,235034839	1

Table 3.8. T-test values for MCF10A and MDA-MB-231 cells between different doses at 24, 48 and 72 hours respectively. Dark values indicate significant differences ($p<0.05$ two tail level).

MCF10A 3D 24well	0 uM	0.5 uM	1.5 uM	2.5 uM	5 uM	10 uM
24-48 hrs	0,921331329	0,243318348	0,011351988	0,015885653	0,017115299	0,284525609
48-72hrs	0,955907173	0,009326921	0,000397121	0,000824086	0,059311415	0,229263957
24-72 hrs	0,955633509	0,001318863	3,40809E-05	4,84545E-06	0,008202643	0,046751424

MDA-MB-231 3D 24well	0 uM	0.5 uM	1.5 uM	2.5 uM	5 uM	10 uM
24-48 hrs	0,344599851	0,153610311	0,060829718	0,003418539	0,130713389	0,305984336
48-72 hrs	0,978244367	0,016709961	0,00167125	0,065081156	0,402245835	0,740737927
24-72 uM	0,401143366	0,001392987	1,20268E-05	0,00059399	0,04562854	0,11722513

Table 3.9. T-test values for MCF10A and MDA-MB-231 cells between different time points. Dark values indicate significant differences ($p<0.05$ two tail level)

MCF10A vs. MDA-MB-231 3D 24well	0 uM	0.5 uM	1.5 uM	2.5 uM	5 uM	10 uM
24 hrs	0,994558934	0,927395783	0,337836633	0,263558396	0,762173984	0,863932379
48 hrs	0,375231495	0,80065873	0,192348989	0,403508195	0,801032515	0,974489966
72 hrs	0,332528089	0,105895293	0,179471829	0,105037512	0,656496441	0,313545376

Table 3.10. T-test values between MCF10A and MDA-MB-231 cells at different time points

T-test results showed that there was no significant difference between increasing doses in 3D in 24 well plate except between 5 µM - 10 µM for MDA-MB-231 cells. According to the analysis performed, significant increase was observed between different time points for MCF10A cells except 0.5 µM between 24 – 48 hours and 5 µM between 48 – 72 hours. When time points was compared for MDA-MB-231 cells, significant increase was observed at 0.5 µM, 1.5 µM, 2.5 µM, 5 µM drug doses between some time points, but MDA-MB-231 cells took drug into cells within 24 hours predominantly. MCF10A and MDA-MB-231 cells showed similarity in terms of intensity values in 3D 24 well plate system.

3.8. Analysis of Effect of Doxorubicin in 3D Cultured Cells on Chip

MDA-MB-231 and MCF10A cells were seeded into 3D microenvironment after mixing 1:1 matrigel. The LOCs were prepared with magnetic paper and final concentration of the cells was $3x10^6$ cells / ml. Drug doses were applied after two days incubation. Different concentrations of doxorubicin (0, 0.5µM, 1.5µM, 2.5µM, 5µM, 10µM) were applied in the MCF10A medium through medium reservoirs and observations were performed after 24, 48 and 72 hours. For 3D microenvironment, Z-stack imaging was performed along the height of the chip. With Z-stack images received, it was confirmed that the 3D microenvironment was provided. From the images obtained from different points, cells were drawn from the phase-contrast photos and obtained ROIs were applied to doxorubicin photos. From each photos, an area that did not contain cell was selected as background, and the intensity of that area was subtracted for intensity calculation.

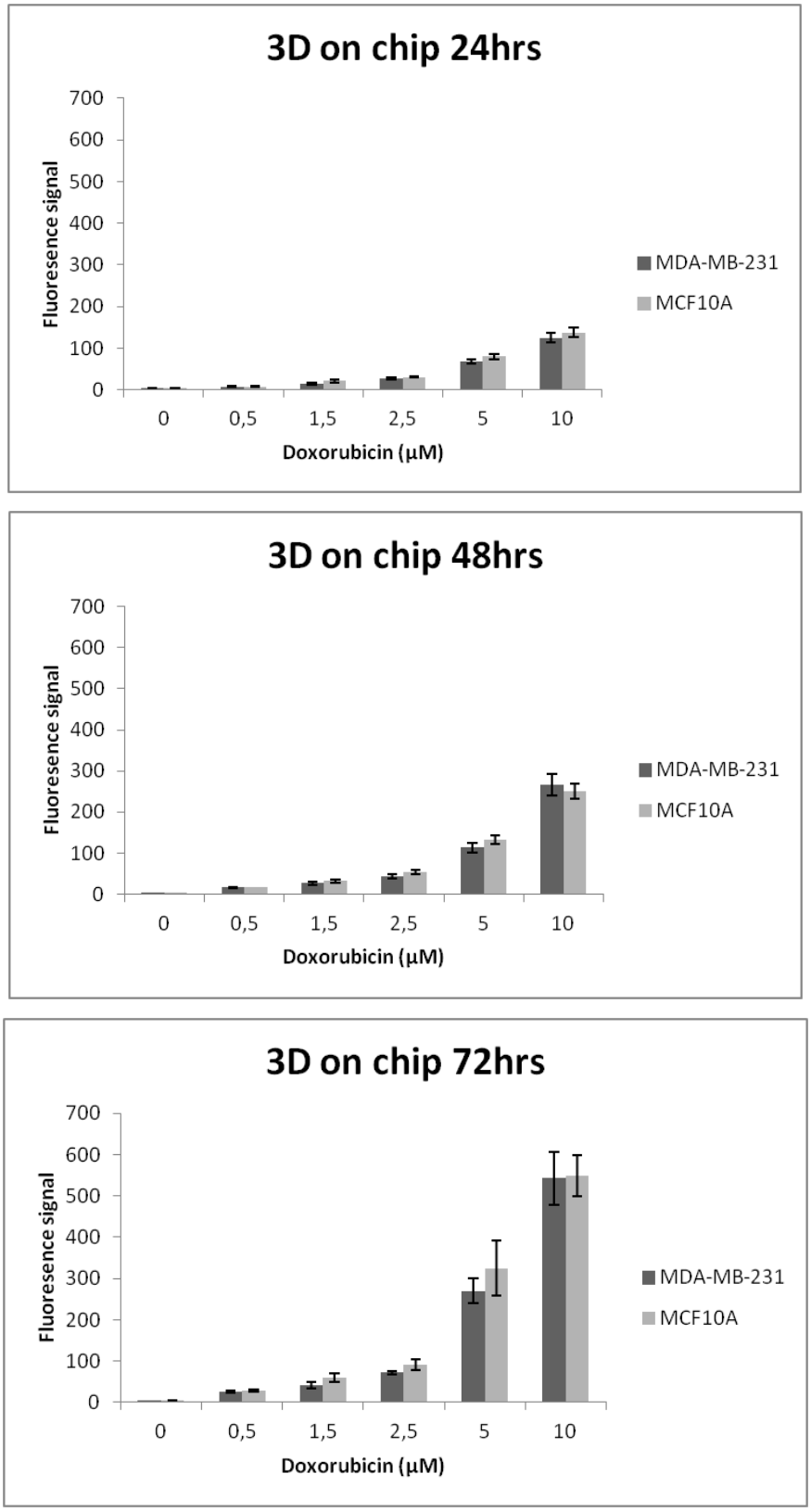

Figure 3.23. Fluorescence signals of MDA-MB-231 and MCF10A cells in 3D LOC system at 24, 48 and 72 hours respectively.

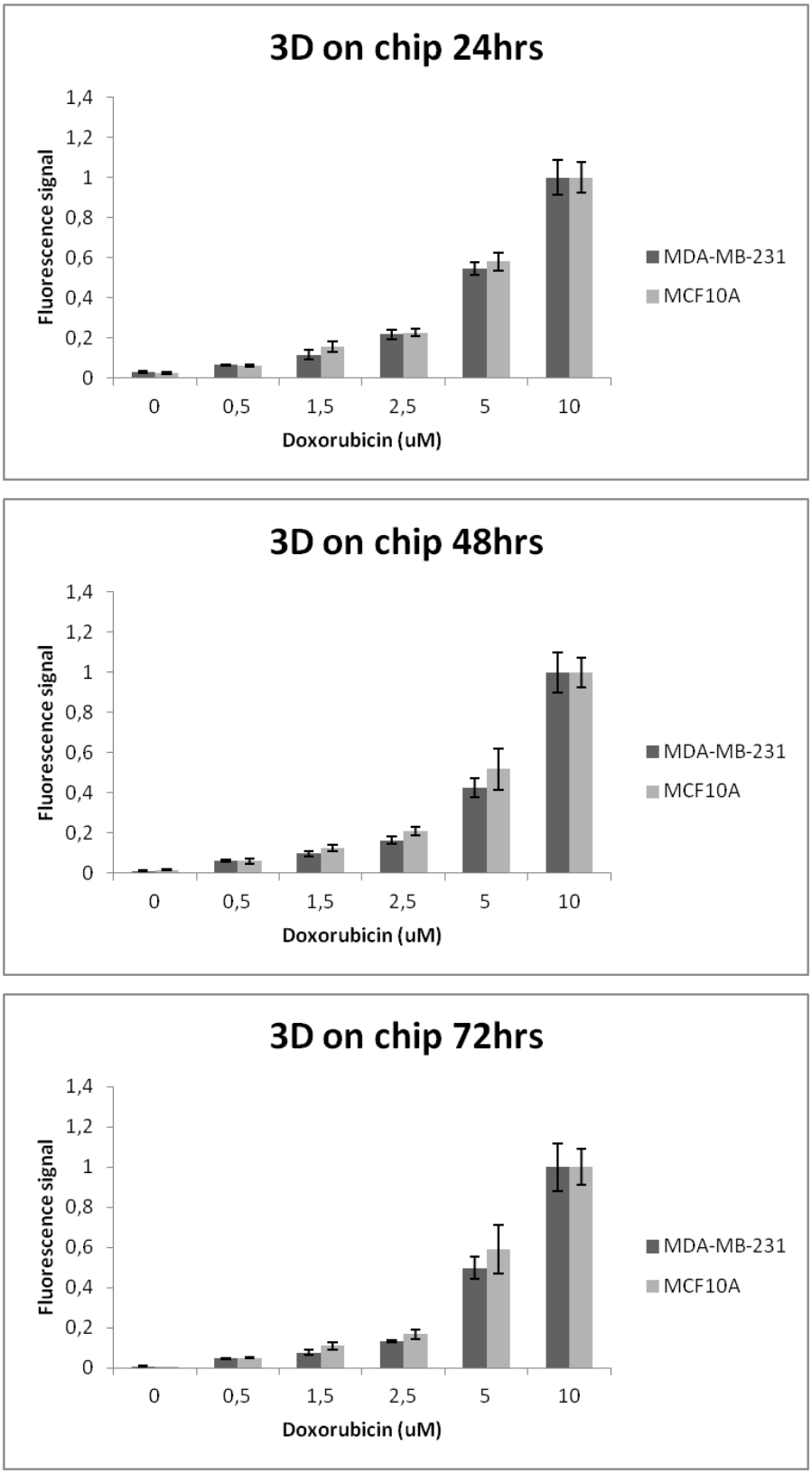

Figure 3.24. Normalized to highest fluorescence signals of each group

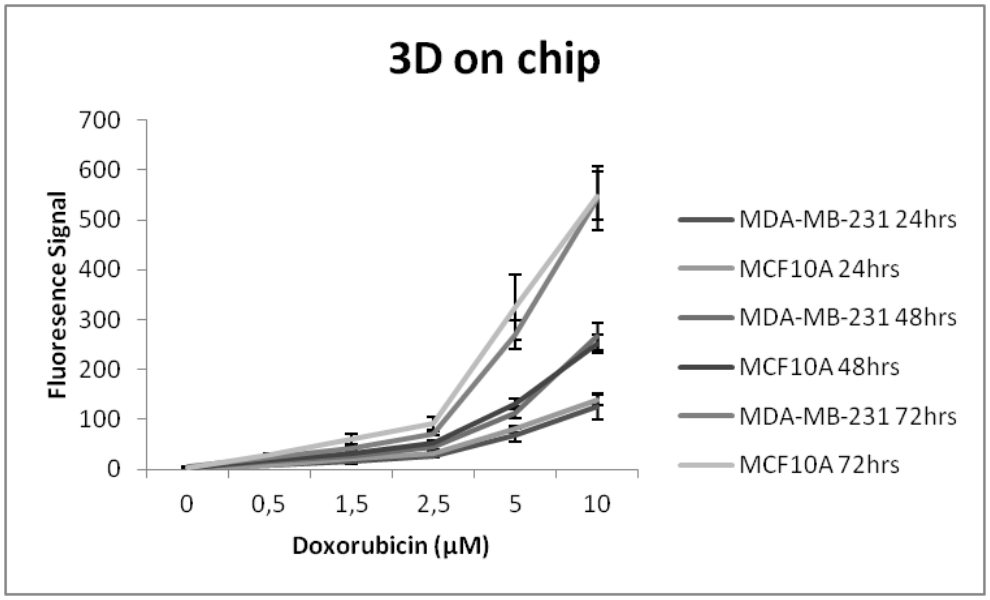

Figure 3.25. Fluorescence signals of MDA-MB-231 and MCF10A cells in 3D LOC system with variation of time and concentration of doxorubicin.

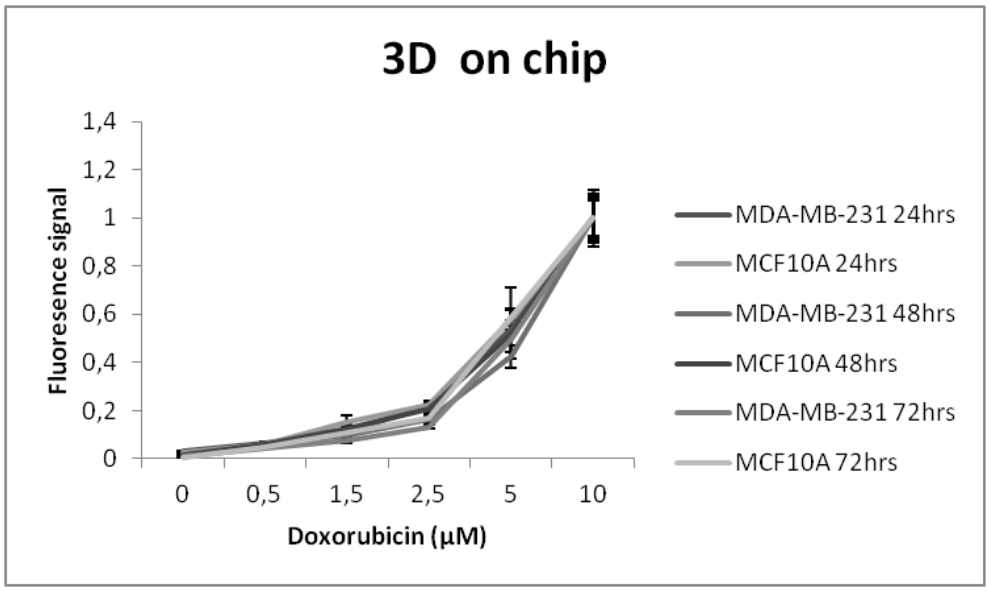

Figure 3.26. Normalized to highest fluorescence signals of each group

MCF10A 24h 3D CHIP	0 uM	0,5 uM	1,5 uM	2,5 uM	5 uM	10 uM
0 uM	1	0,000492783	0,008288121	6,79224E-05	0,000247022	0,001070341
0,5 uM	0,000492783	1	0,024771944	0,000180818	0,000321257	0,001195863
1,5 uM	0,008288121	0,024771944	1	0,048862234	0,000173146	0,000483574
2,5 uM	6,79224E-05	0,000180818	0,048862234	1	0,000693729	0,002247973
5 uM	0,000247022	0,000321257	0,000173146	0,000693729	1	0,00538191
10 uM	0,001070341	0,001195863	0,000483574	0,002247973	0,00538191	1

MDA-MB-231 24h 3D CHIP	0 uM	0,5 uM	1,5 uM	2,5 uM	5 uM	10 uM
0 uM	1	0,000524242	0,021500563	0,001338271	9,44979E-05	0,001475165
0,5 uM	0,000524242	1	0,096079016	0,002823751	0,000122184	0,001641817
1,5 uM	0,021500563	0,096079016	1	0,013886555	1,236E-05	0,002128398
2,5 uM	0,001338271	0,002823751	0,013886555	1	7,269E-05	0,003037858
5 uM	9,44979E-05	0,000122184	1,236E-05	7,269E-05	1	0,007547167
10 uM	0,001475165	0,001641817	0,002128398	0,003037858	0,007547167	1

MCF10A 48h 3D CHIP	0 uM	0,5 uM	1,5 uM	2,5 uM	5 uM	10 uM
0 uM	1	0,019568631	0,00251765	0,00090181	0,007850758	0,00017627
0,5 uM	0,019568631	1	0,013617506	0,000926079	0,011124522	0,000221949
1,5 uM	0,00251765	0,013617506	1	0,016806128	0,01896284	0,000306904
2,5 uM	0,00090181	0,000926079	0,016806128	1	0,041643887	0,000144835
5 uM	0,007850758	0,011124522	0,01896284	0,041643887	1	0,006409451
10 uM	0,00017627	0,000221949	0,000306904	0,000144835	0,006409451	1

MDA-MB-231 48h 3D CHIP	0 uM	0,5 uM	1,5 uM	2,5 uM	5 uM	10 uM
0 uM	1	0,000139238	0,002408539	0,003037068	0,000856452	0,000628322
0,5 uM	0,000139238	1	0,040876157	0,010281455	0,001424872	0,000770889
1,5 uM	0,002408539	0,040876157	1	0,021110474	0,001019162	0,000921597
2,5 uM	0,003037068	0,010281455	0,021110474	1	0,003179049	0,001263492
5 uM	0,000856452	0,001424872	0,001019162	0,003179049	1	0,00213891
10 uM	0,000628322	0,000770889	0,000921597	0,001263492	0,00213891	1

MCF10A 72h 3D CHIP	0 uM	0,5 uM	1,5 uM	2,5 uM	5 uM	10 uM
0 uM	1	0,001157755	0,004539492	0,002463829	0,008325099	0,000389076
0,5 uM	0,001157755	1	0,02474758	0,008382187	0,010927693	0,000466046
1,5 uM	0,004539492	0,02474758	1	0,086773167	0,016660801	0,000638376
2,5 uM	0,002463829	0,008382187	0,086773167	1	0,026118226	0,00029746
5 uM	0,008325099	0,010927693	0,016660801	0,026118226	1	0,030231832
10 uM	0,000389076	0,000466046	0,000638376	0,00029746	0,030231832	1

MDA-MB-231 72h 3D CHIP	0 uM	0,5 uM	1,5 uM	2,5 uM	5 uM	10 uM
0 uM	1	0,001452626	0,006117444	8,77713E-05	0,00085555	0,001095634
0,5 uM	0,001452626	1	0,076843975	2,81182E-05	0,001178876	0,001273706
1,5 uM	0,006117444	0,076843975	1	0,007217435	0,001676885	0,001468262
2,5 uM	8,77713E-05	2,81182E-05	0,007217435	1	0,002683203	0,001832783
5 uM	0,00085555	0,001178876	0,001676885	0,002683203	1	0,008274404
10 uM	0,001095634	0,001273706	0,001468262	0,001832783	0,008274404	1

Table 3.11. T-test values for MCF10A and MDA-MB-231 cells between different doses at 24, 48 and 72 hours respectively. Dark values indicate significant differences ($p<0.05$ two tail level).

MCF10A 3D CHIP	0 uM	0.5 uM	1.5 uM	2.5 uM	5 uM	10 uM
24-48 hrs	0,550324153	9,18126E-06	0,089965965	0,014750927	0,003897315	0,001764032
48-72 hrs	0,973237433	0,025959625	0,043465338	0,006217458	0,044878356	0,002468597
24-72 hrs	0,458092644	0,002654303	0,013518207	0,009877773	0,021189714	0,001263223

MDA-MB-231 3D CHIP	0 uM	0.5 uM	1.5 uM	2.5 uM	5 uM	10 uM
24-48 hrs	0,444050478	0,001201307	0,028122811	0,017488677	0,005076757	0,004741864
48-72 hrs	0,10992324	0,025499282	0,098608912	0,038464711	0,004546	0,010546102
24-72 hrs	0,442091387	0,003039775	0,015986604	4,86816E-05	0,002512869	0,003012151

Table 3.12. T-test values for MCF10A and MDA-MB-231 cells between different time points. Dark values indicate significant differences ($p<0.05$ two tail level)

MCF10A vs. MDA-MB-231 3D CHIP	0 uM	0.5 uM	1.5 uM	2.5 uM	10 uM
24 hrs	0,645680974	0,951707265	0,18556621	0,29319983	0,436166769
48 hrs	0,381795782	0,455477027	0,338637652	0,245404882	0,665644475
72 hrs	0,443381383	0,474753991	0,16402672	0,191099199	0,94748859

Table 3.13. T-test values between MCF10A and MDA-MB-231 cells at different time points

The intensity values of doxorubicin in the cells (MDA-MB-231 and MCF10A) were evaluated depending on the dosage and the time. There was no significant difference between uptake of the doxorubicin between two cell lines, while fluorescence intensity increased according to the doxorubicin dosage and time. These results showed that both time and dosage determined drug uptake predominantly in 3D LOC system.

3.9. Comparison of 2D in 24 well plate & chip

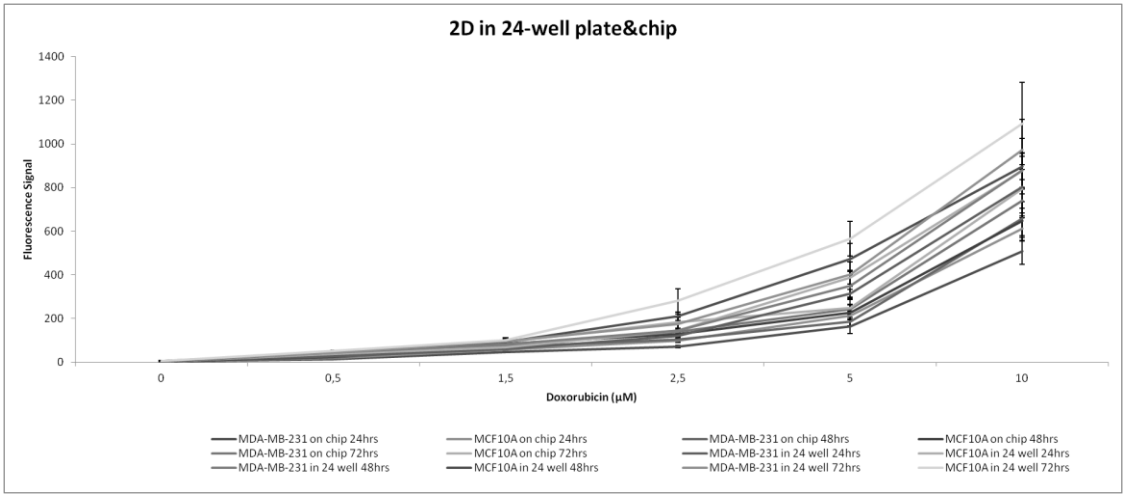

Figure 3.27. Fluorescence signals of MDA-MB-231 and MCF10A cells in 2D in 24 well-plate & on chip at 24, 48 and 72 hours

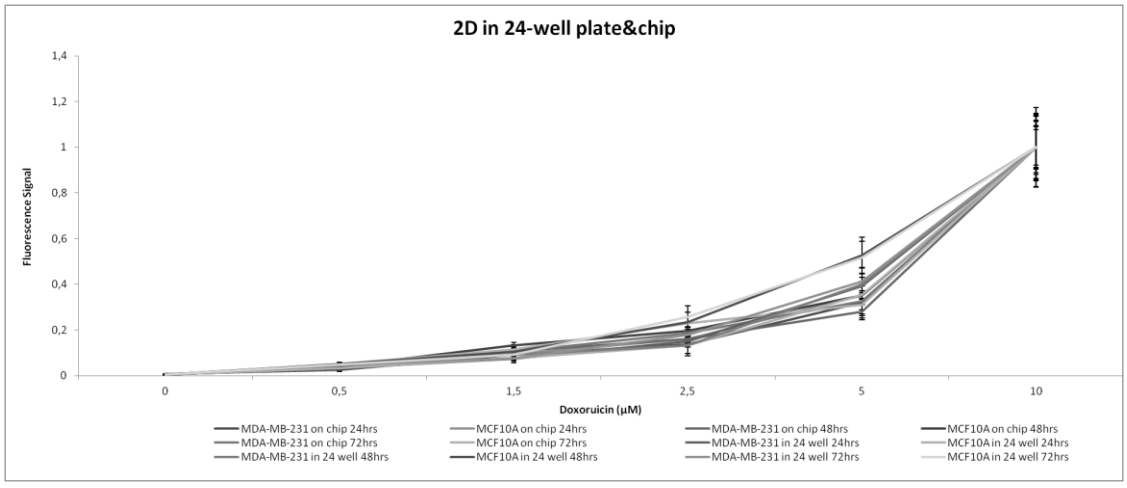

Figure 3.28. Normalized to highest fluorescence signals of each group

MCF10A 2D CHIP vs. 2D 24well	0 uM	0.5 uM	1.5 uM	2.5 uM	5 uM	10 uM
24 hrs	0,414945333	0,038526665	0,3274639	0,002929985	0,030483872	0,034784153
48 hrs	0,378217787	0,063610688	0,616996996	0,007455639	0,027979079	0,150929979
72 hrs	0,235753401	0,016227795	0,684451985	0,165549927	0,016670193	0,2020086

MDA-MB-231 2D CHIP vs. 2D 24well	0 uM	0.5 uM	1.5 uM	2.5 uM	5 uM	10 uM
24 hrs	0,658495491	0,013405323	0,240623386	0,005845929	0,016569389	0,114475682
48 hrs	0,645022525	0,059485791	0,534831639	0,330172151	0,056316914	0,079812706
72 hrs	0,587003377	0,374843879	0,412471463	0,353182995	0,06327604	0,178409305

Table 3.14. T-test values obtained from comparison of MCF10A and MDA-MB-231 cells in 2D 24 well plate and 2D chip. Dark values indicate significant differences ($p<0.05$ two tail level).

When 2D cell culture was compared in 24 well plate and chip, in fluorescence signal there were significant differences mostly at 24 hours. For MCF10A cells significant differences were observed for 0.5 µM, 2.5 µM, 5 µM, 10 µM drug concentrations at 24 hours, 2.5 µM, 5 µM drug concentrations at 48 hours, 0.5 µM, 5 µM drug concentrations at 72 hours. MDA-MB-231 cells showed similarity in both systems at 48 hours and 72 hours, but at 24 hours for 0.5 µM, 2.5 µM and 5 µM MDA-MB-231 cells took drug more in 24 well plate. 2D environment produced in chip allowed a more controlled environment to systematically observe the drug effects using low volume of materials. According to normalized values no significant difference in uptake was observed as a function of dose.

3.10. Comparison of 3D in 24 well plate & chip

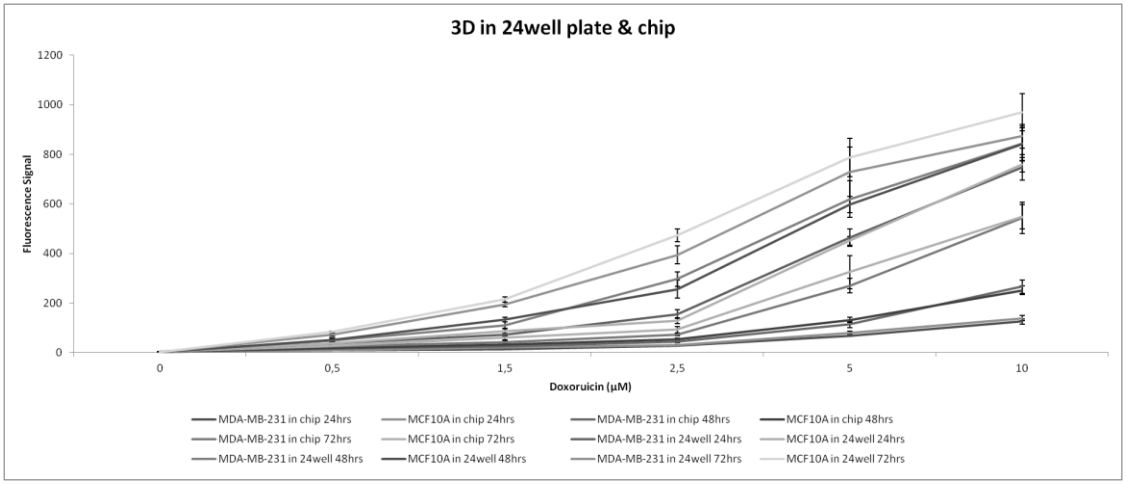

Figure 3.29. Fluorescence signals of MDA-MB-231 and MCF10A cells in 3D in 24 well-plate & on chip at 24, 48 and 72 hours

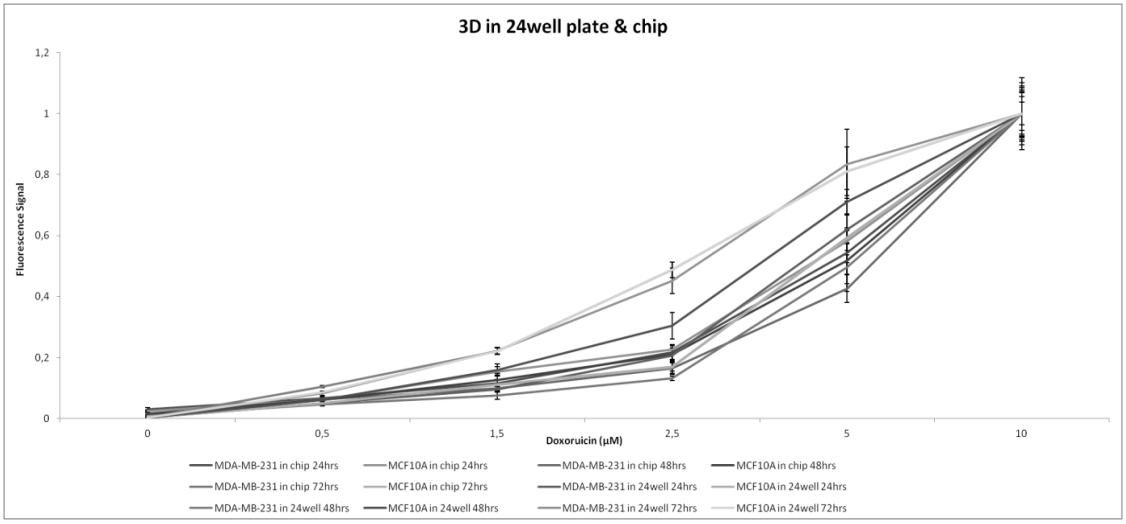

Figure 3.30. Normalized to highest fluorescence signals of each group

MCF10A 3D CHIP vs. 3D 24well	0 uM	0.5 uM	1.5 uM	2.5 uM	5 uM	10 uM
24 hrs	0,21792303	0,011766629	0,003247784	0,000400525	4,71871E-06	8,94405E-07
48 hrs	0,120425059	0,013206958	5,20235E-05	0,002693472	0,000182519	0,000127095
72 hrs	0,019517514	1,78871E-06	4,65265E-06	2,90936E-06	0,001413437	0,002306775

MDA-MB-231 3D CHIP vs. 3D 24well	0 uM	0.5 uM	1.5 uM	2.5 uM	5 uM	10 uM
24 hrs	0,119970245	0,003187917	6,38909E-05	0,002151088	0,000370432	0,001267164
48 hrs	0,678426356	0,004769605	0,004859037	0,000384112	0,006718578	0,000606469
72 hrs	0,046560128	0,000301163	3,59128E-06	0,00031168	0,004484701	0,00449524

Table 3.15. T-test values obtained from comparison of MCF10A and MDA-MB-231 cells in 2D 24 well plate and 2D chip. Dark values indicate significant differences ($p<0.05$ two tail level).

Comparison of 3D cell culture in 24 well plate and chip showed significant differences in terms of drug uptake for both cell lines. Cells characteristics changed and cells took drug significantly more in 24 well plate for all doses and time points. Normalized values showed different trends in uptake as a function of dose.

3.11. Comparison of 2D & 3D in 24 well plate

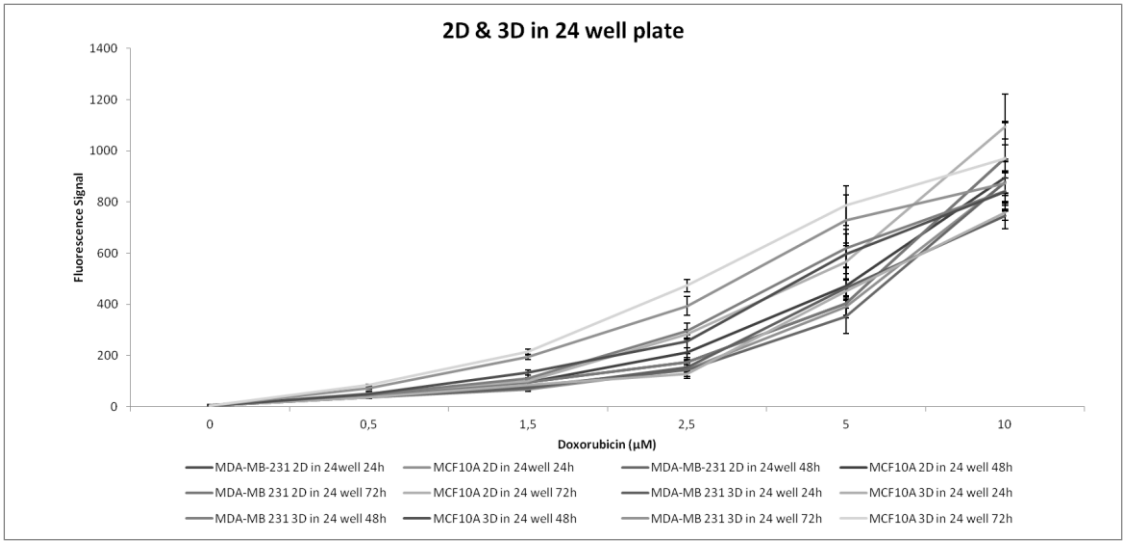

Figure 3.31. Fluorescence signals of MDA-MB-231 and MCF10A cells 2D & 3D in 24 well plate at 24, 48 and 72 hours

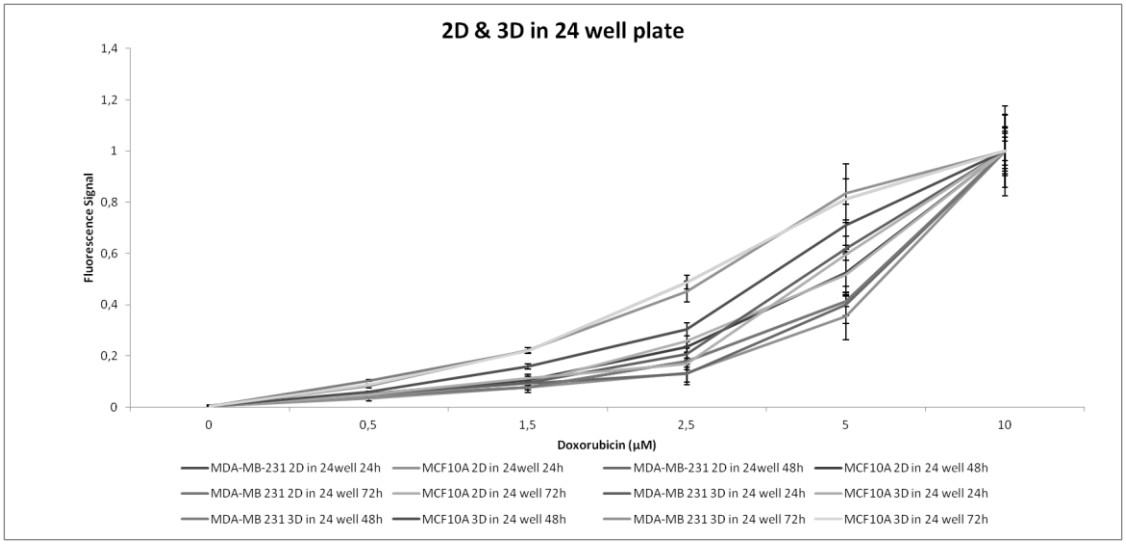

Figure 3.32. Normalized to highest fluorescence signals of each group

2D vs. 3D in 24well MCF10A	0 uM	0.5 uM	1.5 uM	2.5 uM	5 uM	10 uM
24 hrs	0.184468384	0.920760022	0.226553954	0.29492365	0.078928306	0.14944077
48 hrs	0.124642274	0.621003354	0.022425648	0.295313666	0.106486467	0.654045181
72 hrs	0.0840832	4.85002E-05	1.9547E-05	0.004882861	0.052903261	0.495462869

2D vs. 3D in 24well MDA-MB-231	0 uM	0.5 uM	1.5 uM	2.5 uM	5 uM	10 uM
24 hrs	0.244233157	0.099264297	0.229697443	0.145691428	0.011263454	0.670010584
48 hrs	0.344239849	0.529321499	0.169576884	0.004052731	0.025736043	0.710892637
72 hrs	0.244921175	0.007819982	7.62609E-05	0.000852304	0.02068391	0.434625847

Table 3.16. T-test values obtained from comparison of MCF10A and MDA-MB-231 cells 2D in 24 well plate and 3D in 24 well plate. Dark values indicate significant differences ($p<0.05$ two tail level).

According to analyses performed, there was significant difference in drug uptake between 2D in 24 well plate and 3D in 24 well plate for both cell lines. When the intensity values were compared at 24 hours, cells were similar in drug uptake in both two systems except for MDA-MB-231 cells at 5 µM drug dose. According to 48 hours results 1.5 µM for MCF10A cells, 2.5 µM and 5 µM for MDA-MB-231 cells showed differences. At 72 hours high concentration of drug caused similarity in drug uptake. The intensity values normalized to highest fluorescence signals of each group showed different trends about increasement properties.

3.12. Comparison of 2D & 3D on chip

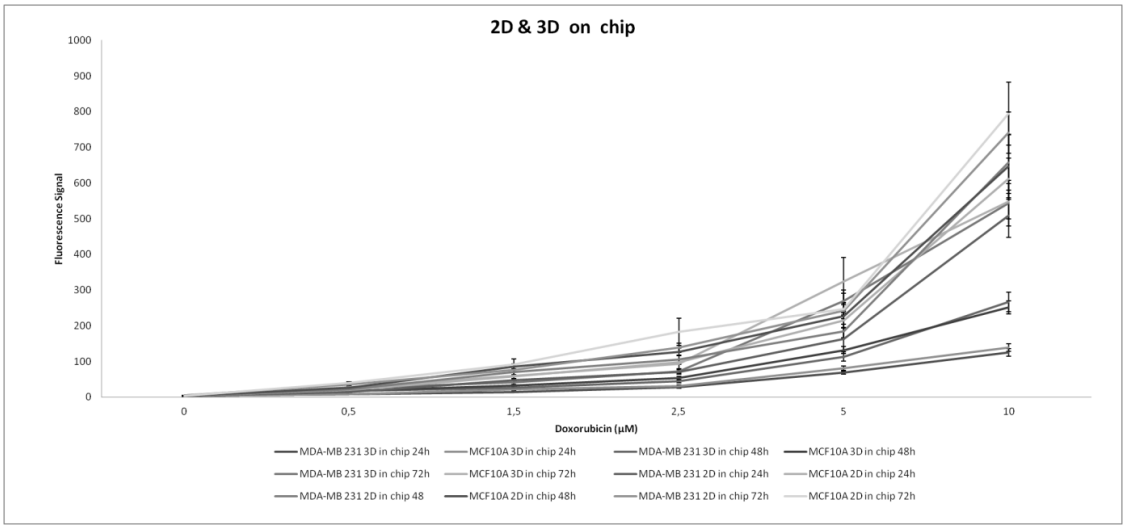

Figure 3.33. Fluorescence signals of MDA-MB-231 and MCF10A cells in 2D & 3D in chip at 24, 48 and 72 hours

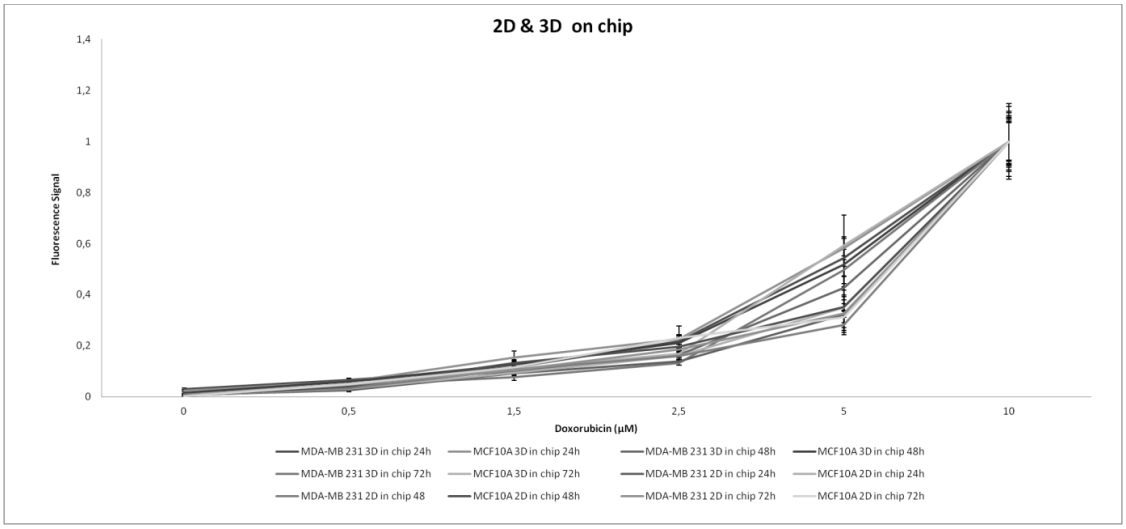

Figure 3.34. Normalized to highest fluorescence signals of each group

2D vs. 3D in CHIP MCF10A	0 uM	0.5 uM	1.5 uM	2.5 uM	5 uM	10 uM
24 hrs	0.48384443	0.018548217	0.00065112	0.000359536	0.072436386	0.001295455
48 hrs	0.285665042	0.019156464	0.001059592	0.000576854	9.40513E-05	0.011935311
72 hrs	0.12248481	0.014593955	0.118491102	0.07274692	0.310468178	0.051882526

2D vs. 3D in CHIP MDA-MB-231	0 uM	0.5 uM	1.5 uM	2.5 uM	5 uM	10 uM
24 hrs	0.662258384	0.241287197	2.58248E-05	0.002565295	0.075208666	0.007322334
48 hrs	0.829860339	0.358843235	0.00606763	0.003832983	0.017400963	0.005146853
72 hrs	0.524383243	0.231192675	0.097544897	0.004591775	0.644244012	0.050244482

Table 3.17. T-test values obtained from comparison of MCF10A and MDA-MB-231 cells 2D in chip and 3D in chip. Dark values indicate significant differences ($p<0.05$ two tail level).

When 2D and 3D cell culture were compared in chip, significant differences were observed between these two systems for both MCF10A and MDA-MB-231 cells. Normalized graph showed similar increase properties. While no significant difference was observed between those systems at 0.5 µM for MDA-MB-231 cells, MCF10A cells took drug into the cells (at 0.5 µM drug concentration) less in 3D microenvironment. Differences between 2D and 3D were more pronounced in chip than in 24 well plate.

3.13. Cell Viability Assay for Cells on Classical and Cell-on-a-chip Culture

To observe cell viability after drug treatment DAPI was used as a fluorescent stain. DAPI concentration was determined 14 µM and applied to the cells after drug treatment at 24, 48 and 72 hours. Staining time was optimized and it was observed that, in five minutes DAPI only passes through and stain death cell nucleus. After this duration, live cells were stained by DAPI. For this reason, pictures were taken in five minutes after DAPI treatment for cell viability assay.

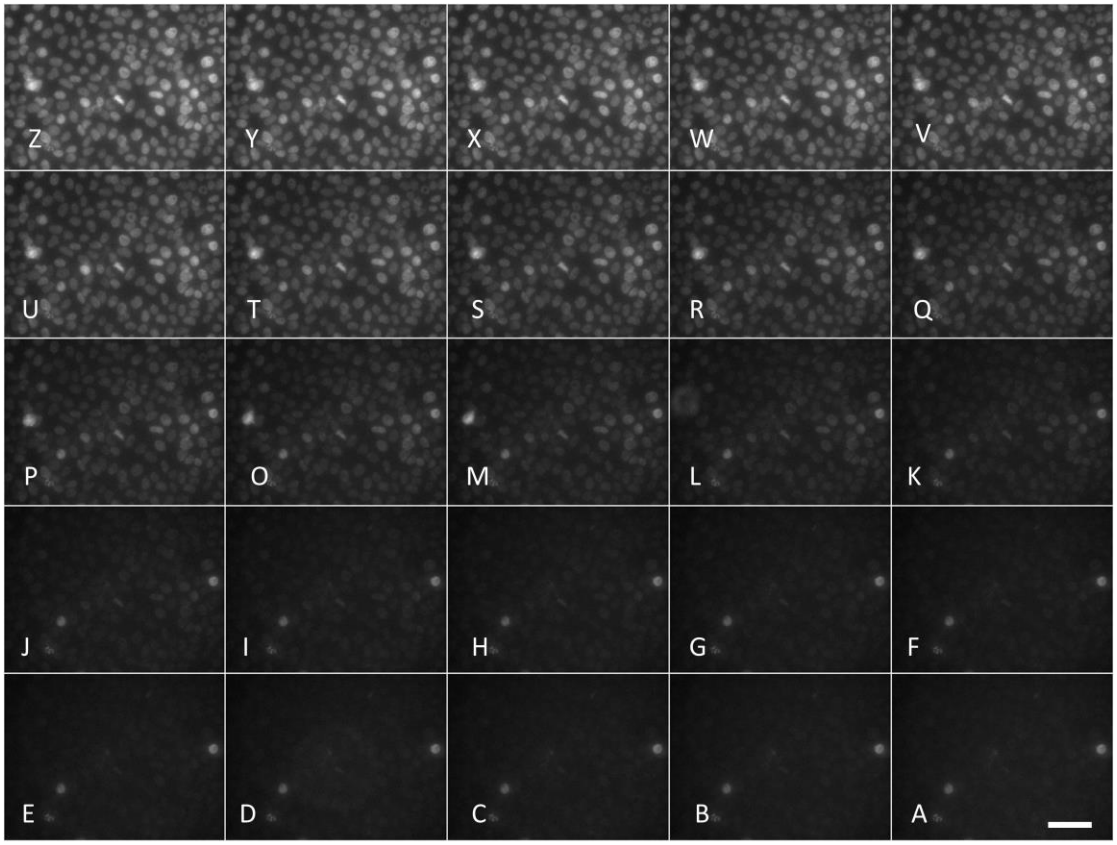

Figure 3.35. DAPI images of MCF10A cells with no drug treatment in 24 well plate. From A to Z pictures were taken intervals of one minute. Scale is 50 µm.

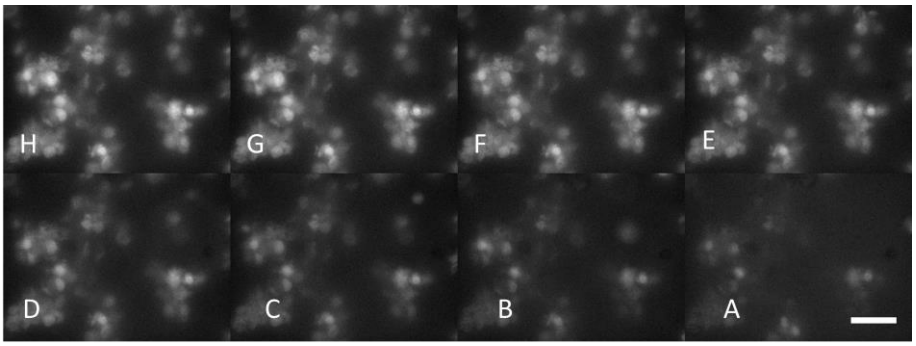

Figure 3.36. DAPI images of MCF10A cells after 10 µM drug treatment in 24 well plate. From A to H pictures were taken intervals of one minute. Scale is 50 µm.

For cell viability assay, cells were seeded in 24 well plate and chip. Only 2D cell culture sytems were formed in these systems. After two days incubation, drug doses were applied and DAPI treatment was performed at different time points. To analyze effect of the drug DOX mean intensity and DAPI mean intensity was used.

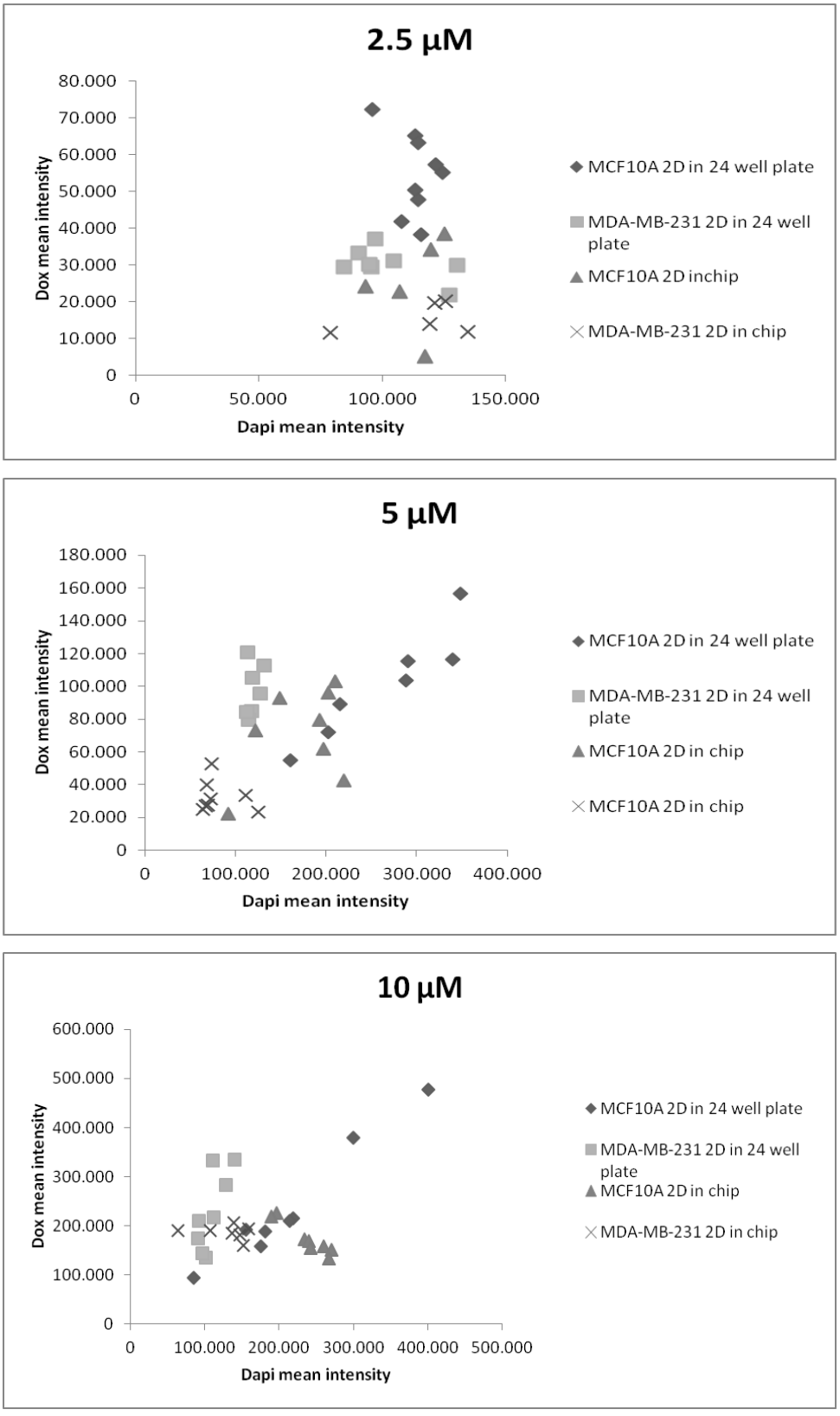

Figure 3.37. Scatter plot of DAPI mean intensity and DOX mean intensity values after 2.5 µM, 5µM and 10 µM drug treatment respectively in 2D 24 well plate and 2D chip

Figure 3.37 shows that DOX intensity and DAPI intensity in the cells increased with doses. More drug uptake into the cells caused the more DAPI signal. When 2D systems were compared after drug treatment, DAPI signal was the highest in 2D 24 well plate. According to drug uptake trials there was no significant differences between MCF10A and MDA-MB-231 cells, but cell viability assay showed that MDA-MB-231 cells were more resistant to die than MCF10A cells.

CHAPTER 4

CONCLUSION

In this study, two and three dimensional cell-on-a-chip culture microenvironments created as an alternative to 24 well system to use in drug studies. Effect of anticancer drug doxorubicin was observed using these microenvironments. For trials, metastatic breast cancer cell line MDA-MB-231 was used to observe the effect of the drug and normal mammary epithelial cell line MCF10A was used for side effects.

For fabrication of two dimensional microenvironment, silicon wafer mold in desired shape and height was prepared using UV lithography technique and channels were formed using PDMS. To convert PDMS to a surface that cell can attach, only poly-L-lysine, only fibronectin and poly-L-lysine + fibronectin coating were tried. After trying various concentrations of fibronectin, it was decided that chips should be covered with first poly-L-lysine and then fibronectin at 0.0125 mg/ml concentration. Incubation durations and cell numbers were tried that would allow cells to be confluent within the chip. 3×10^6 cells / ml cell concentration with 6 hours incubation was decided for further two dimensional cell-on-a-chip experiments. For three dimensional experiments, magnetic paper mold was used to produce 22 chip at once with desired shape and size. Matrigel was used as extracellular matrix to provide three dimensional cell culture. Cell viability in chip was confirmed for over seven days and co-culture medium was determined as MCF10A medium.

To investigate the drug uptake and cell viability in those produced systems, a commonly used anticancer drug doxorubicin and DAPI were used. After cells were seeded at in 24 well plate and chip as two dimensional and three dimensional, they have incubated for two days and after drug treatment images were taken at 24, 48 and 72 hours to assess the drug effect on the two cell lines within the systems.

Experiments performed in four different environments showed no significant difference of drug uptake between metastatic breast cancer cell line MDA-MB-231 and normal mammary epithelial cell line MCF10A. According to cell viability trials MDA-MB-231 cells were more resistant than MCF10A cells to die. This shows the

importance of targeted design and use of anticancer drugs in cancer drug studies and treatment.

In 2D 24 well plate while evaluating the fluorescence signal depending on time, after administration of drug to MCF10A and MDA-MB-231 cells, there was no significant differences of drug uptake into the cell at different time points (24,48, 72 hours). These results showed that in 24-well system, the drug entered into the cell boundries at high proportion within the first 24 hours.

Time dependent differences of drug uptake were observed after treatment with some doses in 2D on chip. While fluorescence signal was lower for some concentrations compared to 24 well plate, generally no significant difference between concentrations was observed at 72 hours. Two dimensional microenvironment in chip required less reagent volume for trials and allowed more controlled and systematic observations compared to 24 well system.

According to analyses performed, MCF10A cells in 3D environment in 24 well plate showed significant differences between 24, 48 and 72 hours. MDA-MB-231 cells took drug into the cell mostly at 24 hours, significant differences was observed between 24 and 72 hours. At high concentration of drug treatment, drug uptake could not increase with time for MDA-MB-231 cells.

Significant differences were observed in drug uptake for both MCF10A and MDA-MB-231 cells in 3D in chip after drug treatment at different time points. Fluorescence signals increased with both drug concentration and time.

When we compare drug uptake into the cells in 24 well plate and chip systems significant differences were observed. In 2D environment, response of MCF10A cells was different in these two systems. MCF10A cells took drug into the cell less in chip than 24 well plate, whereas response of MDA-MB-231 cells were similar. In 3D environment, response of both cell lines were different and drug uptake was lower in chip. When 2D and 3D cell culture was compared, differences between 2D and 3D were more pronounced in chip than in 24 well plate.

Cell viability assay showed that drug uptake and cell viability was not correlated directly. Although both cell lines did not show significant difference in terms of drug uptake, MDA-MB-231 cells showed more resistance to die.

In conculusion, it was clearly seen that according to fluorescence signal intensity in these four different cell culture environment of cells, extracellular matrix and environment change drug effects. Besides lab-on-a-chip systems provide us more

controllable condition and less liquid volume consumption. The most importantly, 3D cell culture system in chip appears to be the most appropriate platform for drug testing.

REFERENCES

Aoudjit, F., & Vuori, K. (2001). Integrin signaling inhibits paclitaxel-induced apoptosis in breast cancer cells. *Oncogene, 20*(36), 4995-5004.

Bar-On, O., Shapira, M. a., & Hershko, D. D. (2007). Differential effects of doxorubicin treatment on cell cycle arrest and Skp2 expression in breast cancer cells. *Anti-cancer drugs, 18*(10), 1113-1121.

Beebe, D. J., Mensing, G. A., & Walker, G. M. (2002). Physics and applications of microfluidics in biology. *Annual review of biomedical engineering, 4*(1), 261-286.

Bélanger, M. C., & Marois, Y. (2001). Hemocompatibility, biocompatibility, inflammatory and in vivo studies of primary reference materials low-density polyethylene and polydimethylsiloxane: A review. *Journal of biomedical materials research, 58*(5), 467-477.

Bischel, L. L., Young, E. W., Mader, B. R., & Beebe, D. J. (2013). Tubeless microfluidic angiogenesis assay with three-dimensional endothelial-lined microvessels. *Biomaterials, 34*(5), 1471-1477.

Bissell, M. J., Radisky, D. C., Rizki, A., Weaver, V. M., & Petersen, O. W. (2002). The organizing principle: microenvironmental influences in the normal and malignant breast. *Differentiation, 70*(9-10), 537-546.

Breslin, S., & O'Driscoll, L. (2013). Three-dimensional cell culture: the missing link in drug discovery. *Drug discovery today, 18*(5), 240-249.

Carpenter, P. M., Dao, A. V., Arain, Z. S., Chang, M. K., Nguyen, H. P., Arain, S., . . . Wilczynski, S. P. (2009). Motility induction in breast carcinoma by mammary epithelial laminin 332 (laminin 5). *Molecular Cancer Research, 7*(4), 462-475.

Correia, A. L., & Bissell, M. J. (2012). The tumor microenvironment is a dominant force in multidrug resistance. *Drug Resistance Updates, 15*(1), 39-49.

Danen, E. H. (2013). Integrin signaling as a cancer drug target. *ISRN Cell Biology, 2013*.

Esmaeilsabzali, H., Beischlag, T. V., Cox, M. E., Parameswaran, A. M., & Park, E. J. (2013). Detection and isolation of circulating tumor cells: Principles and methods. *Biotechnology Advances, 31*(7), 1063-1084. doi:10.1016/j.biotechadv.2013.08.016

Ferlay, J., Soerjomataram, I., Dikshit, R., Eser, S., Mathers, C., Rebelo, M., . . . Bray, F. (2015). Cancer incidence and mortality worldwide: sources, methods and major patterns in GLOBOCAN 2012. *International Journal of Cancer, 136*(5), E359-E386.

Fidler, I. J. (2003). The pathogenesis of cancer metastasis: the'seed and soil'hypothesis revisited. *Nature Reviews Cancer, 3*(6), 453-458.

Ghallab, Y. H., & Badawy, W. (2010). *Lab-on-a-chip: techniques, circuits, and biomedical applications*. Artech House

Godugu, C., Patel, A. R., Desai, U., Andey, T., Sams, A., & Singh, M. (2013). AlgiMatrix™ based 3D cell culture system as an in-vitro tumor model for anticancer studies. *Plos One, 8*(1), e53708.

Goodman, T. T., Ng, C. P., & Pun, S. H. (2008). 3-D tissue culture systems for the evaluation and optimization of nanoparticle-based drug carriers. *Bioconjugate chemistry, 19*(10), 1951-1959. doi:10.1021/bc800233a

Hall, C. L., Dubyk, C. W., Riesenberger, T. A., Shein, D., Keller, E. T., & van Golen, K. L. (2008). Type I Collagen Receptor (α(2)β(1)) Signaling Promotes Prostate Cancer Invasion through RhoC GTPase. *Neoplasia (New York, N.Y.), 10*(8), 797-803.

Hickman, J. A., Graeser, R., de Hoogt, R., Vidic, S., Brito, C., Gutekunst, M., . . . Consortium, I. P. (2014). Three-dimensional models of cancer for pharmacology and cancer cell biology: Capturing tumor complexity in vitro/ex vivo. *Biotechnology Journal, 9*(9), 1115-1128. doi:10.1002/biot.201300492

Huang, C., Park, C. C., Hilsenbeck, S. G., Ward, R., Rimawi, M. F., Wang, Y.-c., . . . Schiff, R. (2011). β1 integrin mediates an alternative survival pathway in breast cancer cells resistant to lapatinib. *Breast Cancer Research, 13*(4), 1.

Huh, D., Hamilton, G. A., & Ingber, D. E. (2011). From 3D cell culture to organs-on-chips. *Trends in cell biology, 21*(12), 745-754.

Huh, D., Matthews, B. D., Mammoto, A., Montoya-Zavala, M., Hsin, H. Y., & Ingber, D. E. (2010). Reconstituting organ-level lung functions on a chip. *Science, 328*(5986), 1662-1668.

Hutmacher, D. W. (2010). Biomaterials offer cancer research the third dimension. *Nature Materials, 9*(2), 90-93.

Hutmacher, D. W., Loessner, D., Rizzi, S., Kaplan, D. L., Mooney, D. J., & Clements, J. A. (2010). Can tissue engineering concepts advance tumor biology research? *Trends in biotechnology, 28*(3), 125-133.

Jaeger, A. A., Das, C. K., Morgan, N. Y., Pursley, R. H., McQueen, P. G., Hall, M. D., . . . Gottesman, M. M. (2013). Microfabricated polymeric vessel mimetics for 3-D cancer cell culture. *Biomaterials, 34*(33), 8301-8313.

Joyce, J. A., & Pollard, J. W. (2009). Microenvironmental regulation of metastasis. *Nature Reviews Cancer, 9*(4), 239-252.

Kang, L., Chung, B. G., Langer, R., & Khademhosseini, A. (2008). Microfluidics for drug discovery and development: from target selection to product lifecycle management. *Drug discovery today, 13*(1), 1-13.

Kenny, P. A., Lee, G. Y., Myers, C. A., Neve, R. M., Semeiks, J. R., Spellman, P. T., . . . Petersen, O. W. (2007). The morphologies of breast cancer cell lines in three-dimensional assays correlate with their profiles of gene expression. *Molecular oncology, 1*(1), 84-96.

Kiefer, J., & Farach-Carson, M. (2001). Type I collagen-mediated proliferation of PC3 prostate carcinoma cell line: implications for enhanced growth in the bone microenvironment. *Matrix Biology, 20*(7), 429-437.

Languino, L. R., Gehlsen, K. R., Wayner, E., Carter, W. G., Engvall, E., & Ruoslahti, E. (1989). Endothelial cells use alpha 2 beta 1 integrin as a laminin receptor. *The Journal of cell biology, 109*(5), 2455-2462.

Lee, M.-Y., Kumar, R. A., Sukumaran, S. M., Hogg, M. G., Clark, D. S., & Dordick, J. S. (2008a). Three-dimensional cellular microarray for high-throughput toxicology assays. *Proceedings of the National Academy of Sciences, 105*(1), 59-63.

Lee, M.-Y., Kumar, R. A., Sukumaran, S. M., Hogg, M. G., Clark, D. S., & Dordick, J. S. (2008b). Three-dimensional cellular microarray for high-throughput toxicology assays. *Proceedings of the National Academy of Sciences of the United States of America, 105*(1), 59-63. doi:10.1073/pnas.0708756105

Levental, K. R., Yu, H., Kass, L., Lakins, J. N., Egeblad, M., Erler, J. T., . . . Weninger, W. (2009). Matrix crosslinking forces tumor progression by enhancing integrin signaling. *Cell, 139*(5), 891-906.

Lovitt, C. J., Shelper, T. B., & Avery, V. M. (2015). Evaluation of chemotherapeutics in a three-dimensional breast cancer model. *Journal of Cancer Research and Clinical Oncology, 141*(5), 951-959. doi:10.1007/s00432-015-1950-1

Lown, J. W. (1993). Anthracycline and anthraquinone anticancer agents: current status and recent developments. *Pharmacology & therapeutics, 60*(2), 185-214.

McBeath, R., Pirone, D. M., Nelson, C. M., Bhadriraju, K., & Chen, C. S. (2004). Cell shape, cytoskeletal tension, and RhoA regulate stem cell lineage commitment. *Developmental cell, 6*(4), 483-495.

Mehta, G., Hsiao, A. Y., Ingram, M., Luker, G. D., & Takayama, S. (2012). Opportunities and challenges for use of tumor spheroids as models to test drug delivery and efficacy. *Journal of Controlled Release, 164*(2), 192-204.

Menendez, J. A., Vellon, L., Mehmi, I., Teng, P. K., Griggs, D. W., & Lupu, R. (2005). A novel CYR61-triggered 'CYR61-αvβ3 integrin loop'regulates breast cancer cell survival and chemosensitivity through activation of ERK1/ERK2 MAPK signaling pathway. *Oncogene, 24*(5), 761-779.

Menke, A., Philippi, C., Vogelmann, R., Seidel, B., Lutz, M. P., Adler, G., & Wedlich, D. (2001). Down-regulation of E-cadherin gene expression by collagen type I and type III in pancreatic cancer cell lines. *Cancer Research, 61*(8), 3508-3517.

Milane, L., Duan, Z., & Amiji, M. (2011). Role of hypoxia and glycolysis in the development of multi-drug resistance in human tumor cells and the establishment of an orthotopic multi-drug resistant tumor model in nude mice using hypoxic pre-conditioning. *Cancer Cell Int, 11*(1), 1.

Miyamoto, H., Murakami, T., Tsuchida, K., Sugino, H., Miyake, H., & Tashiro, S. (2004). Tumor-stroma interaction of human pancreatic cancer: acquired resistance to anticancer drugs and proliferation regulation is dependent on extracellular matrix proteins. *Pancreas, 28*(1), 38-44.

Nguyen, N.-T., Shaegh, S. A. M., Kashaninejad, N., & Phan, D.-T. (2013). Design, fabrication and characterization of drug delivery systems based on lab-on-a-chip technology. *Advanced drug delivery reviews, 65*(11), 1403-1419.

Nicolini, A., Giardino, R., Carpi, A., Ferrari, P., Anselmi, L., Colosimo, S., . . . Berti, P. (2006). Metastatic breast cancer: an updating. *Biomedicine & Pharmacotherapy, 60*(9), 548-556.

Paguirigan, A. L., & Beebe, D. J. (2008). Microfluidics meet cell biology: bridging the gap by validation and application of microscale techniques for cell biological assays. *BioEssays, 30*(9), 811-821.

Park, J. S., Chu, J. S., Tsou, A. D., Diop, R., Tang, Z., Wang, A., & Li, S. (2011). The effect of matrix stiffness on the differentiation of mesenchymal stem cells in response to TGF-β. *Biomaterials, 32*(16), 3921-3930.

Pathak, A., & Kumar, S. (2012). Independent regulation of tumor cell migration by matrix stiffness and confinement. *Proceedings of the National Academy of Sciences, 109*(26), 10334-10339.

Placzek, M. R., Chung, I.-M., Macedo, H. M., Ismail, S., Blanco, T. M., Lim, M., . . . Yeo, D. C. (2009). Stem cell bioprocessing: fundamentals and principles. *Journal of the Royal Society Interface, 6*(32), 209-232.

Sackmann, E. K., Fulton, A. L., & Beebe, D. J. (2014). The present and future role of microfluidics in biomedical research. *Nature, 507*(7491), 181-189.

Schrader, J., Gordon-Walker, T. T., Aucott, R. L., van Deemter, M., Quaas, A., Walsh, S., . . . Iredale, J. P. (2011). Matrix stiffness modulates proliferation, chemotherapeutic response, and dormancy in hepatocellular carcinoma cells. *Hepatology, 53*(4), 1192-1205.

Sethi, T., Rintoul, R. C., Moore, S. M., MacKinnon, A. C., Salter, D., Choo, C., . . . Strieter, R. (1999). Extracellular matrix proteins protect small cell lung cancer cells against apoptosis: a mechanism for small cell lung cancer growth and drug resistance in vivo. *Nature medicine, 5*(6), 662-668.

Siegel, R., Naishadham, D., & Jemal, A. (2012). Cancer statistics, 2012. *CA: a cancer journal for clinicians, 62*(1), 10-29.

Singh, S. S. (2006). Preclinical Pharmacokinetics: An Approach Towards Safer and Efficacious Drugs. *Current Drug Metabolism, 7*(2), 165-182. doi:10.2174/138920006775541552

Smith, C. (2007). Tools for drug discovery: Tools of the trade. *Nature, 446*(7132), 219-222.

Sodunke, T. R., Turner, K. K., Caldwell, S. A., McBride, K. W., & Reginato, M. J. (2007). Micropatterns of Matrigel for three-dimensional epithelial cultures. *Biomaterials, 28*(27), 4006-4016.

Soman, P., Kelber, J. A., Lee, J. W., Wright, T. N., Vecchio, K. S., Klemke, R. L., & Chen, S. (2012). Cancer cell migration within 3D layer-by-layer microfabricated photocrosslinked PEG scaffolds with tunable stiffness. *Biomaterials, 33*(29), 7064-7070.

Song, J. W., & Munn, L. L. (2011). Fluid forces control endothelial sprouting. *Proceedings of the National Academy of Sciences, 108*(37), 15342-15347.

Sung, K. E., Yang, N., Pehlke, C., Keely, P. J., Eliceiri, K. W., Friedl, A., & Beebe, D. J. (2011). Transition to invasion in breast cancer: a microfluidic in vitro model enables examination of spatial and temporal effects. *Integrative Biology, 3*(4), 439-450.

Sanyal S. (2014). Culture and assay systems used for 3D cell culture.

Toplin, I. (1959). A tissue culture cytotoxicity test for large-scale cancer chemotherapy screening. *Cancer Research, 19*(9), 959.

Tsai, M., Kita, A., Leach, J., Rounsevell, R., Huang, J. N., Moake, J., . . . Lam, W. A. (2012). In vitro modeling of the microvascular occlusion and thrombosis that occur in hematologic diseases using microfluidic technology. *The Journal of clinical investigation, 122*(1), 408-418.

Tsui, J. H., Lee, W., Pun, S. H., Kim, J., & Kim, D.-H. (2013). Microfluidics-assisted in vitro drug screening and carrier production. *Advanced drug delivery reviews, 65*(11), 1575-1588.

van de Waterbeemd, H., & Gifford, E. (2003). ADMET in silico modelling: towards prediction paradise? *Nat Rev Drug Discov, 2*(3), 192-204.

Walsh, C. L., Babin, B. M., Kasinskas, R. W., Foster, J. A., McGarry, M. J., & Forbes, N. S. (2009). A multipurpose microfluidic device designed to mimic microenvironment gradients and develop targeted cancer therapeutics. *Lab on a Chip, 9*(4), 545-554.

Wartenberg, M., Frey, C., Diedershagen, H., Ritgen, J., Hescheler, J., & Sauer, H. (1998). Development of an intrinsic P-glycoprotein-mediated doxorubicin resistance in quiescent cell layers of large, multicellular prostate tumor spheroids. *International Journal of Cancer, 75*(6), 855-863.

Webb, B. A., Chimenti, M., Jacobson, M. P., & Barber, D. L. (2011). Dysregulated pH: a perfect storm for cancer progression. *Nature Reviews Cancer, 11*(9), 671-677.

Wei, L.-Y., & Roepe, P. D. (1994). Low external pH and osmotic shock increase the expression of human MDR protein. *Biochemistry, 33*(23), 7229-7238.

Westwood, S. M., Jaffer, S., Lui, O. A., & Gray, B. L. (2007). *Thick SU-8 and PDMS three-dimensional enclosed channels for free-standing polymer microfluidic systems.* Paper presented at the 2007 Canadian Conference on Electrical and Computer Engineering.

Whitesides, G. M. (2006). The origins and the future of microfluidics. *Nature, 442*(7101), 368-373.

Xia, Y. N., & Whitesides, G. M. (1998). Soft lithography. *Angewandte Chemie-International Edition, 37*(5), 551-575.

Xu, X., Farach-Carson, M. C., & Jia, X. (2014). Three-dimensional in vitro tumor models for cancer research and drug evaluation. *Biotechnology Advances, 32*(7), 1256-1268.

Xu, X., Sabanayagam, C. R., Harrington, D. A., Farach-Carson, M. C., & Jia, X. (2014). A hydrogel-based tumor model for the evaluation of nanoparticle-based cancer therapeutics. *Biomaterials, 35*(10), 3319-3330.

Zervantonakis, I. K., Hughes-Alford, S. K., Charest, J. L., Condeelis, J. S., Gertler, F. B., & Kamm, R. D. (2012). Three-dimensional microfluidic model for tumor cell intravasation and endothelial barrier function. *Proceedings of the National Academy of Sciences, 109*(34), 13515-13520.

Zhang, Z., & Nagrath, S. (2013). Microfluidics and cancer: are we there yet? *Biomedical microdevices, 15*(4), 595-609.

Zhau, H. E., Goodwin, T. J., Chang, S.-M., Baker, T. L., & Chung, L. W. (1997). Establishment of a three-dimensional human prostate organoid coculture under microgravity-simulated conditions: evaluation of androgen-induced growth and PSA expression. *In Vitro Cellular & Developmental Biology-Animal, 33*(5), 375-380.

Zhou, Z., Wang, J., Cao, R., Morita, H., Soininen, R., Chan, K. M., . . . Tryggvason, K. (2004). Impaired angiogenesis, delayed wound healing and retarded tumor growth in perlecan heparan sulfate-deficient mice. *Cancer Research, 64*(14), 4699-4702.

Zhu, H., Chen, X., Luo, S., Guan, J., Zhang, W., & Zhang, B. (2005). Involvement of hypoxia-inducible factor-1-alpha in multidrug resistance induced by hypoxia in HepG2 cells. *Journal of experimental & clinical cancer research: CR, 24*(4), 565-574.

Zhu, H., Luo, S., Wang, J., Li, X., Wang, H., Pu, W., . . . Zhuang, Z. (2012). Effect of environmental factors on chemoresistance of HepG2 cells by regulating hypoxia-inducible factor-1α. *Chinese Medical Journal, 125*(6), 1095-1103.

Zustiak, S., Nossal, R., & Sackett, D. L. (2014). Multiwell stiffness assay for the study of cell responsiveness to cytotoxic drugs. *Biotechnology and bioengineering, 111*(2), 396-403.